Toxicological effect of single contaminants and contaminant mixtures associated with plant ingredients in novel salmon feeds

Søfteland, Liv; Kirwan, Jennifer; Hori, Tiago S F; Størseth, Trond R.; Sommer, Ulf; Berntssen, Marc H G; Viant, Mark; Rise, Matthew L.; Waagbø, Rune; Torstensen, Bente E.; Booman, Marije; Olsvik, Pål A.

DOI:
10.1016/j.fct.2014.08.008

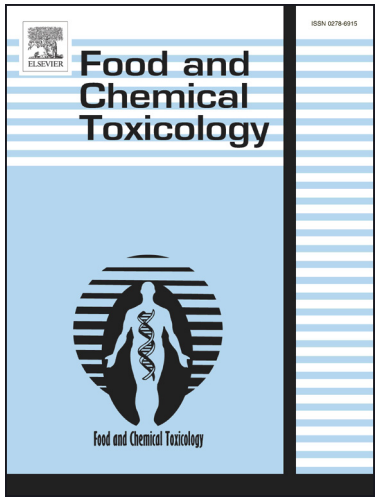

Toxicological effect of single contaminants and contaminant mixtures associated with plant ingredients in novel salmon feeds

Liv Søfteland, Jennifer A. Kirwan, Tiago S.F. Hori, Trond R. Størseth, Ulf Sommer, Marc H.G. Berntssen, Mark R. Viant, Matthew L. Rise, Rune Waagbø, Bente E. Torstensen, Marije Booman, Pål A. Olsvik

PII: S0278-6915(14)00380-9
DOI: http://dx.doi.org/10.1016/j.fct.2014.08.008
Reference: FCT 8072

To appear in: *Food and Chemical Toxicology*

Received Date: 24 February 2014
Accepted Date: 17 August 2014

Please cite this article as: Søfteland, L., Kirwan, J.A., Hori, T.S.F., Størseth, T.R., Sommer, U., Berntssen, M.H.G., Viant, M.R., Rise, M.L., Waagbø, R., Torstensen, B.E., Booman, M., Olsvik, P.A., Toxicological effect of single contaminants and contaminant mixtures associated with plant ingredients in novel salmon feeds, *Food and Chemical Toxicology* (2014), doi: http://dx.doi.org/10.1016/j.fct.2014.08.008

Toxicological effect of single contaminants and contaminant mixtures associated with plant ingredients in novel salmon feeds

Liv Søfteland [a,*], Jennifer A. Kirwan[b], Tiago S.F. Hori[c], Trond R. Størseth[d,] Ulf Sommer[b], Marc H.G. Berntssen[a], Mark R. Viant[b], Matthew L. Rise[c], Rune Waagbø[a], Bente E. Torstensen[a], Marije Booman[c], Pål A. Olsvik [a]

[a] National Institute of Nutrition and Seafood Research, Norway

[b]School of Biosciences, University of Birmingham, UK

[c]Department of Ocean Sciences, Memorial University of Newfoundland, Canada

[d]SINTEF Fisheries and Aquaculture, Norway

*lso@nifes.no

Highlights

Atlantic salmon primary hepatocytes were used to screen for interaction effects caused by PAHs and pesticides.

Lipidomic and transcriptomic profiling suggested perturbation of lipid metabolism and endocrine disruption.

The pesticides gave the strongest responses, despite having less effect on cell viability than the PAHs.

The primary mixture effect was additive.

At high concentrations, the pesticides acted synergistic by decreasing cell viability and down-regulating CYP3A and FABP4.

Toxicological effect of single contaminants and contaminant mixtures associated with plant ingredients in novel salmon feeds

Liv Søfteland [a,*], Jennifer A. Kirwan[b], Tiago S.F. Hori[c], Trond R. Størseth[d,] Ulf Sommer[b], Marc H.G. Berntssen[a], Mark R. Viant[b], Matthew L. Rise[c], Rune Waagbø[a], Bente E. Torstensen[a], Marije Booman[c], Pål A. Olsvik [a]

[a] National Institute of Nutrition and Seafood Research, Norway

[b]School of Biosciences, University of Birmingham, UK

[c]Department of Ocean Sciences, Memorial University of Newfoundland, Canada

[d]SINTEF Fisheries and Aquaculture, Norway

*lso@nifes.no

Abstract

Increasing use of plant feed ingredients may introduce contaminants not previously associated with farming of salmonids, such as pesticides and PAHs from environmental sources or from thermal processing of oil seeds. To screen for interaction effects of contaminants newly introduced in salmon feeds, Atlantic salmon primary hepatocytes were used. The xCELLigence cytotoxicity system was used to select optimal dosages of the PAHs benzo(a)pyrene and phenanthrene, the pesticides chlorpyrifos and endosulfan, and combinations of these. NMR and MS metabolic profiling and microarray transcriptomic profiling was used to identify novel biomarkers. Lipidomic and transcriptomic profiling suggested perturbation of lipid metabolism, as well as endocrine disruption. The pesticides gave the strongest responses, despite having less effect on cell viability than the PAHs. Only weak molecular responses were detected in PAH-exposed hepatocytes. Chlorpyrifos suppressed the synthesis of unsaturated fatty acids. Endosulfan affected steroid hormone synthesis, while benzo(a)pyrene disturbed vitamin D3 metabolism. The primary mixture effect was additive, although at high concentrations the pesticides acted in a synergistic fashion to decrease cell viability and down-regulate CYP3A and FABP4 transcription. This work highlights the usefulness of 'omics techniques and multivariate data analysis to investigate interactions within mixtures of contaminants with different modes of action.

Keywords: Atlantic salmon, PAH, pesticides, metabolomics, synergy, toxicogenomics

1. Introduction

Marine fish oils was traditionally the main source of the persistent organic environmental pollutants (POPs) in salmon feed and farmed Atlantic salmon (*Salmo salar* L.) (Berntssen et al., 2010). Replacing marine ingredients with plant ingredients has reduced the levels of these traditional POPs in salmon feeds, but as a consequence introduced a new cocktail of plant-oil derived contaminants, such as polycyclic aromatic hydrocarbons (PAHs) and pesticides, that have not previously been associated with farming of salmonids (Berntssen et al., 2010; Glover et al., 2007). The introduction of these contaminants to salmon feeds has led to concerns about potential effects on fish health, including interactions with nutritional pathways. Plant oils may be contaminated with PAH during the thermal processing of the oil seeds or indirectly from environmental sources, such as exhaust gases from traffic or from atmospheric particles deposited on the crops during growth (Fromberg et al., 2007; SCF, 2002). The combustion process of oil seeds cause a predominant increase in 2-3 ring PAHs (e.g. phenanthrene), while 4-5 ring PAHs (e.g. benzo(a)pyrene) are present to a lesser extent in the plant crude oils (Teixeira et al., 2007; Dennis et al., 1991). In a feeding trial, a 36% increase of phenanthrene was detected in the fillets of Atlantic salmon fed alternative plant feed (3.2 $\mu g\ kg^{-1}$ or 0.018 µM) compared to fish fed traditional marine fish feed (2.4 $\mu g\ kg^{-1}$ or 0.013 µM). In addition, the levels of benzo(a)pyrene increased from not being detected in the traditional Atlantic salmon fillets to low concentrations being detected (0.3 $\mu g\ kg^{-1}$ or 0.0012 µM) in the plant fed fish fillets (Berntssen et al., 2010). The acute toxicity of PAH in exposed rainbow trout (*Oncorhynchus mykiss*) and largemouth bass (*Micropterus salmonides*) is known to increase with increasing number of aromatic rings (Black et al., 1983). Phenanthrene is therefore considered to have a relatively low toxicity. Phenanthrene is a non-cytochrome P450 1A (CYP1A)-inducing PAH, with aryl hydrocarbon receptor (AhR) independent toxicity (Pathiratne and Hemachandra, 2010; Johnson et al., 2008), while the 4-5 ring PAHs have an AhR dependent mode of action. The main toxicological effects of PAHs, however, are in their genotoxicity and potential endocrine disruption in teleosts (Donnelly and Naufal, 2010; van der Oost et al., 2003; Johnson et al., 2008). Suppressed steroid levels and steroid synthesis inhibition (Monteiro et al., 2000; Seruto et al., 2005;Yan et al., 2012) have been detected in PAH-exposed teleosts as well as retinoid signalling disruption (Benisek et al., 2011).

Endosulfan and chlorpyrifos are pesticides used on crops, and residue levels have been reported in products from plants such as soya or maize (Jergentz et al., 2005; Marchis et al., 2012) that are commonly used as ingredients in salmon feeds (Berntssen et al., 2007). In 2011, the concentration range measured in farmed Atlantic salmon were 0.2-5.8 µg/kg (0.0005-0.014 µM) of α-endosulfan and 0.2-1.2 µg/kg (0.0005-0.003 µM) of β-endosulfan (NIFES, 2014) while chlorpyrifos-methyl has recently been detected in salmon feed (Nácher-Mestre et al., 2014). These pesticides act as endocrine disruptors (Krøvel et al., 2010; Grünfeld and Bonefeld-Jorgensen, 2004). Disturbed steroid production and steroid biosynthesis (Angelis et al., 2009; Viswanath et al., 2010) as well as histopathological changes have been reported in a variety of fish species exposed to chlorpyrifos (Deb and Das, 2012). Adverse effects like liver metabolic perturbations (Ashad et al., 2007; Glover et al., 2007; Krøvel et al., 2000) and disturbed lipid metabolism such as steatosis have been detected in endosulfan exposed Atlantic salmon *in vitro* and *in vivo* (Krøvel et al., 2010; Glover et al., 2007). Elevated ethoxyresorufin O-deethylase activity (EROD) has been observed in endosulfan exposed Atlantic salmon *in vivo* (Glover et al., 2007).

In vitro models are useful supplements to animal models for the evaluation of underlying mechanisms of drugs and contaminants, and for interaction studies (Bouhifd et al., 2012; Xia et al., 2008; Judson et al., 2010; Walum et al., 2005; Søfteland et al, 2011). To ensure optimal non-cytotoxic exposure concentrations for *in vitro* assessments, cell viability and dose-response curves of well-known transcriptional markers are often evaluated (ISO, 2009; Judson et al., 2010; Søfteland et al., 2011). The xCELLigence system use impedance-based, continuous real-time assessment of cytotoxicity and mode of action, and is especially suitable to determine when, and at which concentration, to collect cells for downstream analyses (Xia et al., 2008; Atienzar et al., 2011; Judson et al., 2010;Walum et al., 2005). The xCELLigence system has an equal, or even higher, cytotoxicity sensitivity than the standardised methods certified by ISO (Atienzar et al., 2011; Ceriotti et al., 2007) and has been used in large-scale screening of toxicants (Judson et al., 2010; Xia et al., 2008). In feed safety evaluations, a contaminant-by-contaminant approach has traditionally been applied in the risk assessment. This approach may however be inappropriate in animals exposed to a cocktail of contaminants (Bandele et al., 2012; Kortenkamp and Altenburger, 2011). A toxicological effect of a mixture can be greater (synergistic interaction) or lesser (antagonistic interaction) than expected, and these outcomes are often difficult to predict. This is especially true when mixtures are composed of contaminants with differing modes of action and knowledge

regarding such contaminant mixtures effects is in general lacking (Kortenkamp and Altenburger, 2011).

To gain toxicological knowledge about contaminants found in elevated levels in novel plant-based salmon feeds, the aim of this *in vitro* study was to screen for interaction effects using metabolomic, lipidomic and transcriptomic profiling. To ensure we used non-cytotoxic exposure concentrations, and to find the most potent mixture concentrations, the xCELLigence system was applied for cytotoxicity assessment. RT-qPCR gene expression analysis of well-known and new biomarkers were used for contaminant dose-response determination and interaction evaluation. Atlantic salmon primary hepatocytes were selected as an experimental model.

2. Materials and Methods

2.1 Chemicals

Endosulfan (6,7,8,9,10-hexachloro-1,5,5a,6,9,9,a-hexahydro-6,9-metano-2,4,3-benza-dioxathiepin-3-oxide, α + β ~ 2 + 1; PESTANAL®, analytical standard), chlorpyrifos (O,O-diethyl-O-3,5,6-trichlor-2-pyridyl phosphorothioate, PESTANAL®, analytical standard), phenanthrene (≥98% pure) and benzo(*a*)pyrene **(** ≥96% pure) were all purchased from Sigma-Aldrich (Oslo, Norway). Dimethyl sulfoxide (DMSO) stock solution was purchased from Scientific and Chemical Supplies Ltd. (Bilston, UK), chloroform (HPLC grade) was purchased from Fisher Scientific (Loughborough, UK) and ammonium acetate was purchased from Sigma-Aldrich Co. Ltd (Dorset, UK).

2.2 Isolation of primary cultures of hepatocytes

Juvenile Atlantic salmon (*Salmo salar* L.) were obtained and kept at the animal holding facility at the Institute of Marine Research, Bergen, Norway at Havbruksstasjonen, Matre. The fish were fed once daily with a special feed produced without addition of synthetic antioxidants and with low levels of contaminants, supplied by EWOS, Norway (Harmony Nature Transfer 75). Feed concentrations of chlorpyrifos, endosulfan, benzo(a)pyrene and phenanthrene were all under the level of quantification. All glassware, instruments and solutions were autoclaved prior to liver perfusion. Hepatocytes were isolated from 8 Atlantic salmon (325-515g) with a two-step perfusion method previously described in Søfteland et al. (2009). The final cell pellet was resuspended in L-15 medium containing 10% fish serum (FS) from salmon (Nordic BioSite, Oslo, Norway), 1% glutamax (Invitrogen, Norway) and 1% penicillin-streptomycin-amphotericin (10000 units/ml potassium penicillin, 10000 µg/ml steptomycin sulfate and 25 µg/ml amphotericin B.) (Lonzo, Medprobe, Oslo, Norway). The Trypan Blue exclusion method, performed in accordance with the manufacturer's protocol (Lonzo), was used to determine cell viability. The different cell suspensions used in this study had cell viability between 83-94%. The cell suspensions were plated on 2 µg/cm^2 laminin (Sigma-Aldrich, Oslo, Norway) coated culture plates (TPP, Trasadingen, Switzerland), and the hepatocytes were kept at 10°C in a sterile incubator without additional O_2/CO_2 (Sanyo, CFC FREE, Etten Leur, Netherland). The following cell concentrations were used; 7.2×10^6

cells per well in 6-well plates (in 3 ml complete L-15 medium), 2.6×10^6 cells per well in 12-well plates (in 2 ml complete L-15 medium), 0.2×10^6 cells per well in xCELLigence 96-well plates (in 0.2 ml complete L-15 medium).

2.3 Chemical exposure

The primary cells were cultured for 36-40 hrs prior to chemical exposure with a change of medium (containing 10% FS) after 18-20 hrs. The cells were exposed for 24 hrs to single contaminants, i.e. endosulfan, phenanthrene and benzo(a)pyrene (0.01, 0.1, 1, 10, 100 μM), chlorpyrifos (0.1, 1, 10, 100, 1000 μM) or to simple mixtures of endosulfan, phenanthrene, benzo(a)pyrene and chlorpyrifos according to a factorial experimental design. A full factorial design was used with low (1 μM) and high (100 μM) concentrations, a zero (0.4% DMSO control) concentration, and one centre point (50.5 μM) in order to evaluate linearity (Table 1). The concentrations used for the factorial design were determined from the cell viability and RT-qPCR dose-response curves (Fig. 1-5). 1 μM was chosen as the low concentration for all contaminants due to the up-regulation observed for CYP1A and CYP3A at this concentration by benzo(a)pyrene, endosulfan and chlorpyrifos, in addition to that 1 μM was the lowest concentration that gave a significant cell viability reduction for phenanthrene. The high (100 μM) concentration was chosen since all contaminants, except chlorpyrifos gave a significant cell viability reduction at this concentration and since all contaminants significantly up-regulated vitellogenin (VTG) and/or fatty acid binding protein 4 (FABP4) at this concentration. Cells from three fish were used for cell viability and RT-qPCR dose-response curves evaluation in a preliminary experiment. In a second experiment cell viability, RT-qPCR, metabolomics, lipidomics and microarray analysis were used to evaluate cells toxicological response when exposed to individual contaminants, accordingly to a full factorial design (Table 1) or to selected contaminant mixtures from the design. Cells from five additional fish were employed. The exposure medium contained 1% FS. The exposure medium was substituted with new medium after 18-20 hrs and the chemical exposure was sustained for another 24 hrs. The lowest concentration (0.01 μM) used in the dose-response curves with endosulfan and phenanthrene corresponds to actual levels measured in Atlantic salmon fillets (Berntssen et al., 2010; NIFES, 2014).

193 *2.4 Cytotoxicity testing of chemicals*

194 For the cytotoxicity assessment of the four chemical compounds, real time impedance data
195 obtained by the xCELLigence systems (Roche Diagnostics, Oslo, Norway) was used. The
196 xCELLigence system quantifies electrical impedance across electrodes in 96-well cell culture
197 E-Plates. The impedance measurement gives quantitative information regarding cells'
198 biological status including morphology, cell number and viability. Optimal plate coating
199 conditions and cell density were determined in preliminary experiments (data not shown).
200 After a background reading was measured, the appropriate number of cells was added to the
201 plate. The cells were allowed to attach at room temperature (30 min) before the plate was
202 placed on the xCELLigence plate reader in the cell incubator for continuous impedance
203 recording. The real time cell monitoring was conducted at 10°C in an incubator without
204 additional O_2/CO_2 (Sanyo, CFC FREE, Etten Leur, Netherland), using the RTCA single plate
205 xCELLigence platform. The data was collected with intervals of 2 min after contaminant
206 exposure for 12 hrs, then every 15 min for 120 h. The cell index (CI) is a parameter that is
207 derived from the measured cell-electrode impedance data that quantifies the status of the cells
208 (Abassi et al. 2009). Generally, when cells attach onto the electrodes, the CI value increases.
209 A decrease in CI correlates to cell detachment. However, changes in cell morphology will
210 affect the CI. A normalized CI (NCI) at a specific time point is calculated by dividing the CI
211 at that particular time by the CI of a reference time point which is set to 1. The last time point
212 before compound exposure was used for the normalization, allowing a more precise
213 comparison of the control versus effect of the different contaminant concentrations tested. The
214 CI values presented here were calculated from three or five replicate values. Determination of
215 cytotoxic effects was done according to the International standardised test for in vitro
216 cytotoxicity, ISO 10993-5:2009 (ISO, 2009). Contaminant will be deemed cytotoxic when
217 cells viability exceeds 30% reduction compared to the control.

218

219 *2.5 Metabolomics and lipidomics*

220 *2.5.1 Metabolite extraction and NMR spectroscopy*

221 Lyophilized samples were extracted using a 1145 µl mixture of chloroform:methanol:water
222 (2:2:1.8) and vortexed in 2 ml glass vials. The polar and non-polar phases of this bi-phasic
223 mixture were separated, and the polar phase (500 µl) was vacuum centrifuged (30 min at

300K), frozen and freeze dried, for Nuclear magnetic resonance spectroscopy (NMR) analysis. For the non-polar phase, 300 µl were evaporated under N_2 and stored at -80°C before shipment on dry ice for MS analysis.

Subsequently the dried polar metabolite fraction was resuspended in 200 µl D_2O with 1 mM TMSP and transferred to NMR tubes. All samples were maintained at 277 K and analyzed within 48 hrs of resuspension. NMR was performed on a Bruker DRU 600 NMR spectrometer (600.23 MHz for ^1H) fitted with a 5 mm CPQCI cryogenic probe (Bruker Corporation). Three mm NMR tubes were used with the Bruker Sampletrack autosampler in which the samples were kept at 279 K before (and after) analysis. The spectra were recorded at 300 K with suppression of the residual water resonance using the noesygppr1d pulse sequence from the Bruker pulse sequence library. A pulse width of 7.91 µs was used to collect 128 free induction decays with 32K data points with a spectral window of 12,019 Hz (20 ppm). The acquisition time was 2.73 s and the interscan delay was 3 s. The noesy mixing time was 10 ms. The data were zero filled to 64K and exponential line broadening of 0.3 Hz applied before Fourier transformation. The spectra were phased and baseline corrected.

2.5.2 FT-ICR mass spectrometry

All dried lipid samples were resuspended in an equal volume of 2:1 methanol:chloroform with 5 mM ammonium acetate. Lipidomic analyses were conducted in negative ion mode using a hybrid 7-T FT-ICR mass spectrometer (LTQ FT Ultra, Thermo Fisher Scientific, Bremen, Germany) with a chip-based direct infusion nanoelectrospray ionisation assembly (Triversa, Advion Biosciences, Ithaca, NY). Nanoelectrospray conditions comprised of a 200 nL/min flow rate, 0.4 psi backing pressure and -1.2 kV electrospray voltage controlled by ChipSoft software (version 8.1.0). Mass spectrometry conditions included an automatic gain control setting of 5×10^5 and a mass resolution of 100,000. Analysis time was 4.25 min (per technical replicate), controlled using Xcalibur software (version 2.0, Thermo Fisher Scientific). Spectra were collected using the "SIM stitching" method, i.e. acquisition of fourteen overlapping selected ion monitoring (SIM) mass ranges that were subsequently fused together, ranging from *m/z* 70 to 2000 (Southam et al., 2007, Weber et al., 2011). Each sample was analysed in triplicate. A quality control (QC) sample consisting of a pooled aliquot of the samples was analysed repeatedly throughout the batch of samples.

2.6 Microarray and *Quantitative real-time RT-PCR*

2.6.1 RNA extraction

The RNeasy Plus mini kit (Qiagen, Crawley, UK) was used to extract total RNA according to the manufacturer's protocol. RNA was eluted in 30 µl RNase-free MilliQ H_2O and stored at -80°C. The RNA quantity and quality were assessed with the NanoDrop® ND-1000 UV-Vis Spectrophotometer (NanoDrop Technologies, Wilmington, DE, USA) and the Agilent 2100 Bioanalyzer (Agilent Technologies, Palo Alto, CA, USA) pursuant to the manufacturer's instructions. The integrity of the RNA was evaluated with the RNA 6000 Nano LabChip® kit (Agilent Technologies). The samples used in this experiment had 260/280nm absorbance ratios that varied between 1.76 and 2.41, 260/230 nm ratios above 2 and RNA integrity number (RIN) values above 9.5, which indicate pure RNA and intact samples (Schroeder et al., 2006).

2.6.2 Microarray; target synthesis and microarray hybridization

For experimental samples, anti-sense amino-allyl RNA (aaRNA) was amplified from the original individual column-cleaned total RNA samples using the Message Amp II aRNA Amplification kit (Ambion, Life Technologies, Burlington, ON), following the manufacturer's instructions. Only one round of amplification was necessary and it was carried out with 1 µg of total RNA input. For the common reference, an equal contribution of every sample involved in the experiment was pooled and 1 µg of this pool was used in four amplification reactions. The resulting amplified aaRNA from each reaction was pooled to make a final common reference. Amplified aaRNA quality and quantity was measured using UV spectrophotometry and agarose gel electrophoresis, respectively. Anti-sense amino-allyl RNA was labelled with either Cy3 or Cy5 (GE Healthcare, Mississauga, ON) following the manufacturer's instructions with minor modifications. Twenty µg of amplified aaRNA was precipitated overnight following standard molecular biology procedures and re-suspended in coupling buffer (Ambion, Life Technologies); the resulting solution was used in the labelling reaction following the manufacturer's protocol. Experimental individuals were labelled with Cy5 and the common reference was labelled with Cy3. Labelled aaRNA was purified using

the columns supplied with the kit, and labelling efficiency was measured using the "microarray" function of the NanoDrop (ThermoFisher, Mississauga, ON).

Agilent 4-by-44,000 oligonucleotide probes (4x44K) custom salmonid microarrays designed by the consortium for Genomic Research in All Salmonids Project (cGRASP) (Jantzen et al., 2011) were used in this experiment (GEO accession # GPL11299). Hybridizations were carried out following the manufacturer's instructions using 825 ng of each labelled sample (i.e. one experimental sample and one reference sample) per array and the HI-RPM hybridization buffer (Agilent, Mississauga, ON). Hybridizations were carried out for 16 hrs at 65°C with 10 rpm rotation in an Agilent hybridization oven. Following hybridizations, arrays were washed following the manufacturer's instructions. Arrays were scanned using a Perkin Elmer ScanArray Gx Plus at 5 µm resolution and laser power at 90%. If the average signal intensity between channels was not within 300 photomultiplier tube settings (PMTs) were adjusted to balance the channel in subsequent scans. Fluorescence intensity data was extracted from TIFF image files using Imagene v8.5 (BioDiscovery, El Segundo, CA).

2.6.3 Quantitative real-time RT-PCR

The transcriptional levels of selected target genes were quantified with a two-step real-time reverse transcription polymerase chain reaction (RT-PCR) protocol. A serial dilution curve of total RNA with six points in triplicates between 1000 – 31 ng were made for PCR efficiency calculations. 500 ng of total RNA was added to the reaction for each sample, and reverse transcription (RT) reactions were run in duplicates using 96-well reaction plates. No-template control (ntc) and no-amplification control (nac) reactions were run for quality assessment for every gene assay. The 50 µl RT reactions were performed at 48°C for 60 min utilizing a GeneAmp PCR 9700 thermocycler (Applied Biosystems, Foster City, CA, USA). Individual RT reactions contained 1X TaqMan RT buffer (10X), 5.5 mM $MgCl_2$, 500 mM dNTP (of each), oligo dT primers (2.5 µM), 0.4 U/µl RNase inhibitor and 1.67 U/µl Multiscribe Reverse Transcriptase (Applied Biosystems) and RNase-free water.

For every gene analysed, quantitative real-time RT-PCR (real-time qPCR) was run in 10 µl reactions on a LightCycler® 480 Real-Time PCR System (Roche Applied Sciences, Basel, Switzerland) containing 2.0 µl cDNA (diluted twofold). The real-time qPCR was carried out in two 384-well reaction plates using SYBR Green Master Mix (LightCycler 480 SYBR Green master mix kit, Roche Applied Sciences, Basel, Switzerland) containing gene-specific primers and FastStart DNA polymerase. PCR runs were performed with a 5 min activation and denaturing step at 95°C, followed by 45 cycles with each cycle consisting a 10 s denaturing step at 95°C, a 10 s annealing step and finally a 10 s extension step at 72°C. The primer pairs had an annealing temperature of 60°C; see Table 2 for primer sequences, amplicon sizes and GenBank accession numbers. Final primer concentrations of 500 nM were used. For confirmation of amplification of gene-specific products, a melting curve analysis was carried out and the second derivative maximum method (Tellmann, 2006) was used to determine crossing point (CT) values using the Lightcycler 480 Software. To calculate the mean normalized expression (MNE) of the target genes, the geNorm VBA applet for Microsoft Excel version 3.4 was used to calculate a normalization factor based on three reference genes. By using gene-specific efficiencies calculated from the standard curves, the CT values are converted into quantities (Vandesompele et al., 2002). Elongation factor 1 AB (EF1AB) and acidic ribosomal protein (ARP) and β-actin were the selected reference genes for this experiment. The reference genes were stable with gene expression stability (M) values of 0.38.

2.7 Data analysis

2.7.1 Metabolomics

The processed NMR spectra were imported into Matlab (The Mathworks, Inc.) using Prometab v3.3 software (Viant et al. 2003). The region from 10 to 0.5 ppm was imported with a resolution of 0.02 ppm which resulted in 4750 data points, and transformed using a generalized log transformation. Principal Component Analysis (PCA) and Partial Least Squares Discriminant Analysis (PLS-DA) was performed in PLS-toolbox v7.0.1 (Eigenvector Research, Inc.) on normalized and mean centered data prior to multivariate statistical analyses.

2.7.2 Lipidomics

All analyses were performed in Matlab 7.8.0 with PCA and PLS-DA analysis performed in PLS-toolbox v.6.7.1. Mass spectra were processed using a three-stage filtering algorithm as described in Payne et al. (2009). Samples were subsequently normalised using probabilistic quotient normalisation (Dieterle et al., 2006). Processing the raw mass spectra yielded a dataset that was further optimised using a QC based method as described in Kirwan and Broadhurst et al. (2013). Mass features with over 20% missing values across all samples were removed and the resulting intensity matrix was submitted for univariate statistical analysis as described below. A k-nearest neighbour approach (Hrydziuszko et al 2012) was applied to impute missing values to the same dataset and it was transformed using a generalized log transformation prior to multivariate statistical analysis. The final lipidomics dataset was comprised of 1603 mass features upon which statistical analyses were conducted. PCA and PLSDA were performed to assess the overall effect (http://CRAN-R-project.org). All supervised models were validated using cross validation and permutation testing to avoid over-fitting. Univariate statistical analyses were conducted on the lipidomics dataset. An analysis of variance (ANOVA) followed by Games-Howell (GH) post hoc testing (Games and Howell 1976) was applied across the control and the highest doses of each of the four contaminants using a custom adapted version of freely available Matlab scripts (Trujillo-Ortiz and Hernandez-Walls 2003). ANOVA and GH post hoc testing was also applied across all doses of the contaminant mixtures against control. ANOVA was also applied to compare the control against the low and high doses for each individual contaminant. A Benjamini-Hochberg false discovery correction of 10% was applied to all univariate statistical results (Benjamini and Hochberg 1995).

Lipidomic pathway analysis was conducted according to Kanehisa (2008) utilising pathways listed in the Kyoto Encyclopedia of Genes and Genomes (KEGG) database. For each mass feature, KEGG and MI-Pack software were used to assign a putative empirical formula(e) and identity based on accurate mass. To measure the perturbation of each pathway, the empirical formulae associated with the significantly changing mass features were compared against the total number of detected empirical formulae in that pathway to give a “percent of empirical formulae perturbed” for each treatment.

2.7.2 Microarray data pre-processing and analysis

Data pre-processing and normalization were carried out in R using the mArray package. Print-tip Loess normalization (i.e. per sub-grid), threshold setting and removal of low-quality/flagged spots were done as described in Booman et al. (2011) and Hori et al. (2012). After spot quality filtering, features absent in more than 30% of the arrays were discarded and not used in the analysis, resulting in a final list of 9469 probes. Missing data for the 9469 probes was imputed using LSImpute (Bo et al., 2004; Celton et al., 2010) as previously described (Hori et al., 2012). Differentially expressed genes between controls and exposed groups were identified using the rank products algorithm (Breitling et al., 2004) as implemented in the RankProd (Hong et al., 2006) R package with a percentage of false positives (PFP) of 10%. A Rank Product test is demonstrated to be a robust method for microarray experimental designs with few replicates (Jeffery et al, 2006).

2.7.3 xCELLigence and RT-qPCR data

GraphPad Prism 6.0 software (GraphPad Software Inc., Palo Alto, CA, USA) was used for the statistical analyses of the xCELLigence and the RT-qPCR dose–response curves evaluation using one-way ANOVA followed by a Dunnett's post hoc test ($p < 0.05$) to detect treatment variation in contaminant-exposed hepatocytes. Mean±SE were calculated for three or five replicates. For the statistical analyses of the VTG RT-qPCR dose-response curve, Student's t-test ($p < 0.05$) was used to detect significant difference between the highest chlorpyrifos concentration and the 0.4% DMSO control hepatocyte cell cultures. Regression was performed with PLS (Wold et al., 1984) to correlate the design matrix to the responses of different transcripts. Modde 9.0 (Umetrics, Umeå, Sweden) was used for the experimental design and the PLS analysis. Before the PLS analysis the blend matrix was augmented with interaction terms, the data were scaled to unit variance and mean centred. The PLS models were validated with respect to explained variance and goodness of prediction (shown as Q^2), obtained after cross validation (Wold, 1978). The PLS model was in addition evaluated with respect to goodness of fit (R^2).

3. Results

3.1Cytotoxicity screening and RT-qPCR biomarker screening

3.1.1 Individual exposures

3.1.1.1 Cytotoxicity screening

Primary Atlantic salmon hepatocytes were used to establish cytotoxic dose-response curves for the two individual PAHs benzo(a)pyrene and phenanthrene, and for the two individual pesticides chlorpyrifos and endosulfan. With the xCELLigence cytotoxicity system, phenanthrene (Fig. 1A) was the most potent compound, significantly decreased cell viability of 21%, 25%, and 22% at the three highest exposure concentrations (1-100 µM) respectively. Cell viability was only significantly reduced at the highest exposure concentrations (100 µM) for benzo(a)pyrene with 25% (Fig. 1B) and endosulfan (Fig. 1C) 24% compared to the 0.4% DMSO control. None of the applied chlorpyrifos concentrations (0.1-1000 µM) induced a significant cell viability reduction effects in the hepatocytes (Fig. 1D). No significant difference was found between the medium control and the 0.4% DMSO control, and therefore the medium control was not included in Fig. 1A-1D.

3.1.1.2 RT-qPCR biomarker screening

To ensure we were working in a relevant concentration range for Atlantic salmon primary hepatocytes, dose-response curves were established for the four selected biomarkers CYP1A, CYP3A, VTG and FABP4. Chlorpyrifos (Fig. 2) gave a bell-shaped CYP1A transcript up-regulation pattern, though CYP1A was only significantly up-regulated at 10 µM with a fold change (FC) of 16.8 ($p=0.001$). The CYP3A transcript did not show a clear dose-response however CYP3A was significantly elevated at 0.1 ($p=0.01$) and 10 µM ($p=0.5$) of chlorpyrifos. The FABP4 transcript was significantly expressed at 100 µM chlorpyrifos

(p=0.0001) compared to the control. In similarity to FABP4, the VTG transcript was according to the microarray results (data not shown) significantly induced at the highest chlorpyrifos exposure concentration (100 μM) compared to the control. The ANOVA posthoc analysis of the RT-qPCR data did however not confirm this finding, even though a direct comparison between the control and the 100 μM group using the t-test suggested this difference was significant (VTG, p=0.05). Endosulfan exposure (Fig. 3) gave significant up-regulation of FABP4 (p=0.05) and VTG (p=0.0001) at a concentration of 100 μM, with the VTG transcript showing the highest up-regulations with a FC of 17.3. Benzo(a)pyrene (Fig. 4) up-regulated CYP1A transcription (p=0.0001), most profoundly at 1 μM (FC of 191), with a significant dose-dependent reduction in the expression levels at concentrations of 10 and 100 μM. As for the CYP1A transcript, CYP3A was only significantly up-regulated by benzo(a)pyrene at 1 μM (p=0.001). In addition, benzo(a)pyrene significantly up-regulated VTG at 100 μM (p=0.05). No distinct dose-dependent responses were detected in hepatocytes exposed to phenanthrene (Fig. 5), however, the transcripts CYP1A (p=0.05) and VTG (p=0.001) were significantly induced at the highest concentration (100 μM) investigated. VTG had the highest induction with a FC of 10.9 compared to the control.

Based on the cell viability data obtained with the xCELLigence system and transcriptional dose-response curves obtained with RT-qPCR, a factorial design with non-cytotoxic concentrations of the contaminants, 1 μM (low) and 100 μM (high), were subsequently used in the cytotoxicity mixture toxicity interaction evaluation. The different contaminant mixtures used in the factorial design are presented in Table1.

3.1.2. Mixture exposures

3.1.2.1 Cell viability screening

The different contaminant mixtures gave at the most a cell viability reduction of 12% compared to the control, and contaminant mixture 4 and 16 showed the strongest cell viability reduction effect. PLS analysis was performed on the xCELLigence normalized cell index (NCI) values obtained for mixture exposures to benzo(a)pyrene, phenanthrene, chlorpyrifos and endosulfan according to a factorial design. The PLS model (R^2-value = 0.7 and the Q^2-value 0.4.) had four negative linear terms for benzo(a)pyrene, phenanthrene, chlorpyrifos and

endosulfan, indicating that all chemicals contributed to reduced cell viability, however only two linear terms, for phenanthrene (p=0.029) and endosulfan (p=0.015), were significant (Fig. 6). The model also contained one negative interaction term, for chlorpyrifos and endosulfan which were significant (p=0.031). A contour analysis of the xCELLigence cytotoxicity PLS model indicated a synergistic interaction response between chlorpyrifos and endosulfan in mixture-exposed hepatocytes.

3.2. Metabolic profiling

Cells exposed to DMSO (0.4%), 1 μM (low dose) and 100 μM (high dose) of chlorpyrifos, endosulfan, phenanthrene, and benzo(a)pyrene, and contaminant mixtures 1 (1μM of all contaminants), 4 (100 μM of the PAHs and 1 μM of the pesticides) and 16 (100 μM of all contaminants) were selected to be analysed with metabolomics (water-soluble metabolites) and lipidomics (N=5).

3.2.1 Lipidomics

3.2.1.1 Individual exposures

Unsupervised PCA and supervised PLS-DA data analysis of the lipidomics spectra revealed an apparent separation of the exposed group from the control only at the highest dose (100 μM) of the two concentrations analysed for chlorpyrifos (p=0.007; Fig. 7A and 7B), endosulfan (p=0.014; Fig. 7C and 7D), and benzo(a)pyrene (p=0.005; Fig. 7E and 7F). PCA also demonstrated a separation between the control samples and lowest dose of endosulfan. The ANOVA followed by GH post hoc analysis of the high dose exposures of the individual contaminants revealed that chlorpyrifos induced the greatest number of significantly changing mass features with 92 mass features significantly changing compared to the control. Endosulfan induced the second largest perturbation with 22 significant mass features, followed by benzo(a)pyrene (7 significant mass features). Phenanthrene has been removed from the analysis as it induced only one significant perturbation compared to the control. Fig. 8A characterises the overlap of the significant mass features across the individual contaminant exposure. Benzo(a)pyrene shared no significant mass features with chlorpyrifos and endosulfan, whereas the pesticides had 6 significant mass features in common, making the pesticides more similar in their mode of action.

The KEGG pathway analysis (Table 3) of the individual contaminants revealed 10 potentially perturbed pathways, five of which are linked to fatty acid and cholesterol metabolism. Chlorpyrifos may have an affect on the biosynthesis of unsaturated fatty acids (suppressed several desaturase pathways, e.g. Δ9 and Δ11 desaturases) (Fig. 9A), linoleic acid metabolism (suppressed desaturase and elongase pathways to produce ARA, as well as increased cytochrom P450 pathway eicosanoid production) (Fig. 9B) and arachidonic acids metabolism (increased eicosanoid production) (Fig. 9C). Endosulfan indicates an affect on primary bile acid biosynthesis and steroid biosynthesis (increased levels of cholesterol for steroid hormone biosynthesis and production of VTG) (Fig. 9D) while benzo(a)pyrene mainly appears to affect steroid biosynthesis (affecting vitamin D metabolism, increased levels of vitamin D metabolites) (Fig. 9D).

3.2.1.2 Mixture exposures

The contaminant mixtures induced a higher number of significantly changing mass features ($q<0.1$ by ANOVA, $p<0.05$ by GH), than the individual contaminants except chlorpyrifos. They primarily affected mass features with putative identities that have been linked to the pathways of bile acid biosynthesis and biosynthesis of unsaturated fatty acids. Contaminant mixture 16 induced most changes with 149 significant mass features compared to contaminant mixture 1 with 57 significant mass features and contaminant mixture 4, the least effective inducer, with 39 significant mass features (Fig. 8B). However, when modelling by PLS-DA, only contaminant mixture 4 ($p=0.031$) and contaminant mixture 16 ($p=0.002$) could be reliably distinguished from the other classes.

When comparing the overlap between the significant mass features induced by the high dose of individual contaminants and those induced by the contaminant mixtures, 40% of the mass features induced by the individual contaminants were found to overlap with those induced by the contaminant mixtures (Fig. 8C). When comparing the different contaminant mixtures, 70% of significantly changing mass features were uniquely significantly changed with respect to the control only in contaminant mixture 16 which contained the highest doses of all four contaminants. Despite this, none of the features significant in the comparison of the control

class and mixture 16 were significantly different in more than two of the individual contaminant classes when compared to mixture 16 suggesting that the combination of contaminants caused an additive effect (Table SI1). According to the KEGG pathway analysis, contaminant mixture 16 may affect other pathways not perturbed by the other mixtures but the coverage of these pathways was poor and thus the significance of these perturbations are uncertain. According to the KEGG pathway analysis, contaminant mixtures (Table 3) affected primary bile acid biosynthesis, suppressed biosynthesis of unsaturated fatty acids (Fig. 9 A) and linoleic acid metabolism (Fig. 9B) and steroid biosynthesis (increased levels of cholesterol for steroid hormone biosynthesis and production of VTG) (Fig. 9D).

3.2.2 Metabolomic (water-soluble metabolites)

The PCA and PLS-DA analyses of the polar metabolites showed no significant differences between the control and exposed groups (data not presented).

3.3 Transcriptomic

3.3.1Mixture exposures

3.3.1.1 Microarray analysis

In addition to the lipidomic and metabolomic screening, microarray was used for identification of new biomarkers. Contaminant mixture 4 was used for the microarray experiment since it showed the strongest cell viability reduction of the different contaminant mixtures in the cytotoxicity screening. Top rank product lists of differentially expressed features with PFP below 10% in Atlantic salmon hepatocytes exposed to contaminant mixture 4 (N=5), are presented in Table 4. In total 17 features were significantly regulated with PFP below 10%, all significantly affected features like microtubule-associated proteins 1A/1B light chain 3B precursor (MAP1LC3B), transcription factor SOX-4 (SOX4) and VTG were up-regulated, and VTG (C065R146) showed the strongest response with a FC of 13.19.

3.3.1.2 RT-qPCR Contaminants interaction evaluation of mixtures

PLS analysis was performed on seven transcripts (Table 5) and the expression levels (MNE) obtained in cells exposed to benzo(a)pyrene, phenanthrene, endosulfan and chlorpyrifos using a factorial design in order to determine possible chemical interactions. VTG, MAP1LC3B, SOX4 were chosen as biomarkers due to their expression levels identified with microarray screening, whereas CYP1A, CYP3A, FABP4, and peroxisome proliferator-activated receptor α (PPARα) were all target genes evaluated with RT-qPCR that were not identified with the microarray screening.

The PLS analysis of three transcripts showed no combined effect between the contaminants in the mixture suggesting that only one of the contaminants was driving the observed response. For example, endosulfan (p=0.025) was the only contaminant contributing to VTG up-regulation (R^2=0.658 and Q^2=0.47), despite the fact that the PAHs and the pesticides' singly induced VTG and that the PLS model contained one negative interaction term for chlorpyrifos and endosulfan (p=0.02). The PLS analysis showed that, of the three transcripts that revealed additivity, CYP1A (R^2= 0.93 and the Q^2=0.81) gave the strongest response. However, of the four contaminants only chlorpyrifos (p=0.0001) and endosulfan (p=0.0001) contributed to the additive transcriptional reduction of CYP1A expression levels. The FABP4 (R^2=0.95 and Q^2=0.66) was another transcript where additivity was identified and benzo(a)pyrene (p=0.01), phenanthrene (p=0.034) and chlorpyrifos (p=0.00007) all contributed to this additivity. Chlorpyrifos had the largest regression coefficient, and thus had a larger contribution to positive regulation of FABP4. Further, the model had three significant negative interaction terms. A counterplot of the interaction term between phenanthrene and endosulfan (p=0.022) showed antagonistic interaction at low concentrations. However, the interaction term for chlorpyrifos and endosulfan (p=0.0003) had the largest regression coefficient, and thus had a larger contribution to the regulation of FABP4. The counterplot analysis of this interaction term identified a synergistic interaction between chlorpyrifos and endosulfan on the up-regulation of FABP4 at high concentrations, with increasing phenanthrene concentrations. The PLS model for CYP3A (R^2=0.83 and Q^2=0.49), the second transcripts for which synergistic interactions were identified, had only two significant terms, one negative linear term for endosulfan (p=0.0005) and one negative interaction term for endosulfan and chlorpyrifos (p=0.042). A counterplot analysis of the negative interaction term showed a synergistic interaction between the two pesticides on the reduction of CYP3A at high concentration and with increased concentration of phenanthrene.

3. Discussion

Cytotoxicity assays are extensively used to assess *in vitro* cell viability in fish cell cultures, including to rank chemical toxicity and to evaluate chemical mixtures (Segner and Braunbeck, 2003; Wood et al., 2006). According to the international standard for *in vitro* cytotoxicity testing (ISO, 2009), contaminants are first considered cytotoxic when cell viability are reduced with more than 30%. The four compounds assessed with the xCELLigence system showed only a 0-25% cell viability reduction, therefore, none of the contaminants were cytotoxic in the concentration ranges used in this study. Phenanthrene was the most potent compound, significantly decreasing cell viability with 21-25% at the three highest concentrations (1, 10 and 100 μM). This result is in line with a study of Shirmer et al. (1998) who, in exposed rainbow trout gill cells (RTgill-W1), found that five lighter PAHs with two or three benzene rings, including phenanthrene, gave a stronger cell viability reduction than heavier PAHs such as the five ringed PAH benzo(a)pyrene. Shirmer et al. (1998) suggested that the lipid solubility of heavier PAHs prevents them from being adequately accumulated in cells and membranes. In zebrafish (*Danio rerio)* larvae, phenanthrene and benzo(a)pyrene exposure caused a similar toxic response (Wolinska et al., 2011), suggesting that lighter PAHs can be at least as potent as heavier PAHs.

Similar to benzo(a)pyrene, the endosulfan xCELLigence screening revealed a dose-dependent reduction of cell viability, which was significant only at the highest exposure concentration (100 μM). This result is in line with previous findings obtained with the MTT cell viability test (0.01-100 μM) in endosulfan-exposed Atlantic salmon primary hepatocytes (Krøvel et al., 2010). Compared to endosulfan, none of the applied chlorpyrifos concentrations (0.1-1000 μM) affected cell viability in the exposed hepatocytes. In a cytotoxicity screening with the rainbow trout liver (RTL-W1) and rainbow trout gonadal (RTG-2) cell lines, Babin and Tarazona (2005) found chlorpyrifos (0-8.6 μM) to be the most potent compound of six pesticides tested in a neutral red assay and a FRAME KB protein assay. The reason for this discrepancy in sensitivity between salmonid primary hepatocytes and cell lines to chlorpyrifos is not known.

Lipidomic and transcriptomics profiling were further employed to generate hypotheses about the potential modes of action of the studied contaminant and contaminant mixtures. The contaminant exposure showed that chlorpyrifos had the most dominant effect on the lipodome despite showing no effect on cell viability. Endosulfan induced the second largest perturbation, followed by benzo(a)pyrene, while phenanthrene, the most potent cell viability reducing contaminant, induced no distinct perturbation according to the lipidomics data. Chlorpyrifos appeared to affect pathways associated with linoleic acid metabolism as well as the biosynthesis of unsaturated fatty acids, whereas endosulfan may affect steroid biosynthesis and primary bile acid biosynthesis pathways. Lipids have important physiological functions in fish, such as structural components in cell membranes, in cell signalling, and in storage of cellular energy (Torstensen et al., 2001). Therefore, the down-regulation of the biosynthesis of unsaturated fatty acids suggests that chlorpyrifos, among other pathways, may disturb energy-requiring metabolic mechanisms (LeBlanc et al., 2012). Inhibition of essential linolenic fatty acid metabolism has previously been seen in norflurazon-exposed rat liver cells (Hagve et al., 1985). Earlier studies have shown impaired fatty acid metabolism (Ortiz-Zarragoitia and Cajaraville, 2005) as well as metabolic perturbation by exposure to pesticides like endosulfan and chlorpyrifos (Demur et al., 2013; Wang et al., 2011) and to PAHs (Van Scoy et al., 2010; Lin et al., 2009) in exposed mammals and salmonids.

Although eicosanoids can be difficult to detect since they are normally present at low concentrations in biological samples, several putatively annotated eicosanoids in different lipid metabolism pathways was affected by chlorpyrifos exposure in Atlantic salmon hepatocytes. In the arachidonic acid metabolic pathway the putatively annotated eicosanoid tromboxan (11-dehydro-TXB2), was one of several elevated in the chlorpyrifos exposed primary hepatocytes. 11-dehydro-TXB2 is an intermediate of TXA2, which is a vasoconstrictive eicosanoid that has previously been associated with liver injury (Yokayama et al., 2005). In the linoleic acid metabolism pathway, the putatively annotated eicosanoids 9,12-dihydroxy-epoxyoctadecanoate, a precursor of tetrahydrofurandiols (THF-diols), and TriHOME were elevated by chlorpyrifos exposure. These metabolites are involved in inflammatory reactions, cellular energy metabolism and cell homeostasis (Mickalik and Wahli, 2008; Penigrahy et al., 2010). THF-diols are eicosanoids that are involved in

inflammatory reactions and are produced by cytochrome P-450 epoxidations and epoxide hydrolase (sEH) mediated hydrolysis (Konkel and Schunck, 2011; Moghaddam et al., 1996). Several CYP enzymes like CYP1A1/2 and CYP3A4 take part in linoleic acid cytochrome P450 eicosanoid biosynthesis in mammalian species (Konkel and Schunck, 2011). According to the RT-qPCR data, both CYP1A (17-fold up-regulated) and CYP3A (1.46-fold up-regulated) transcripts were induced in hepatocytes exposed to chlorpyrifos. A similar CYP-induction was not seen in endosulfan-exposed hepatocytes in this study or in an earlier study by Krøvel et al., (2010). CYP1A and CYP3A, via AhR- and PXR-receptor activation respectively, could therefore be responsible for the biotransformation of chlorpyrifos and the fatty acids and the production of lipid THF-diols (Konkel and Schunck, 2011).

The fatty acid binding proteins (FABPs) have an essential role in the regulation of the flux of fatty acid in cells, and FABP4 is a well-established marker for inflammation and metabolic syndrome in humans (Cabre et al., 2007; Terra et al., 2011). The putatively identified FABP that may represent the adipose tissue type FABP (h6FABP or FABP11) in fish, an orthologue to mammalian FABP4 (Torstensen et al., 2009), was induced by both pesticides; with chlorpyrifos being the most potent inducer according to the RT-qPCR data. Endosulfan has previously been shown to cause lipid metabolism disturbances such as steatosis, which is triacylglycerols (TAG) accumulation in liver, in both *in vitro* [i.e. in exposed hepatocyte cultures (Krøvel et al., 2010)] and *in vivo* studies (Glover et al., 2007) involving Atlantic salmon. FABP4 was significantly elevated by endosulfan at 100 µM, the same concentration at which Krøvel et al., (2010) detected accumulation of TAG in endosulfan exposed primary hepatocytes. In humans trophoblasts, increased lipid accumulation was found to be linked to elevated transcription of FABP4 (Duttaroy, 2009; Scifres et al., 2011). FABP4 is transcriptionally activated by the peroxisome proliferator activated receptor γ (PPARγ) (Michalik and Wahli, 2008), which is the key regulator of adipogenesis (Janesick and Blumberg, 2011). Our results therefore suggest that PPARs may be upstream regulators of the response to chlorpyrifos and endosulfan in exposed hepatocytes, explaining the observed effects on eicosanoid lipids and steroids, which is in line with earlier published results (Michalik and Wahli, 2008; Li and Chiang, 2009; Parkinson and Ogilvie, 2008; Peraza et al., 2006).

In pesticide and contaminant mixture exposed cells the lipidomics data revealed that the levels of cholesterol, the precursor of steroid hormone biosynthesis, were higher than in the other

691 exposure groups. An effect on steroid hormone biosynthesis was also suggested by the
692 observed induction of a transcript encoding VTG, the primary egg-yolk precursor protein, by
693 the contaminant mixtures and both pesticides at 100 μM. Endosulfan was the strongest
694 inducer of VTG according to the RT-qPCR data. VTG is normally produced in female fish
695 under estrogenic stimulation of ovarian follicle development (Ekman et al., 2008; Hinton et
696 al., 2008). A number of studies have shown endocrine disruption effects caused by
697 organochlorine and organophosphate pesticides, both possessing the ability to interfere with
698 the estrogen receptor (ER) pathway (Krøvel et al., 2010; Grünfeld and Bonefeld-Jorgensen,
699 2004). The lipid metabolism perturbations induced by endosulfan and chlorpyrifos in male
700 hepatocytes can in part be linked to endocrine disruption due to an increased need for
701 cholesterol for VTG production. Comparable effects have been detected in fish exposed to
702 estrogenic compounds. Earlier fish trials have shown impaired fatty acid metabolism (Ortiz-
703 Zarragoitia and Cajaraville, 2005) and/or effects on cholesterol homeostasis (Bravo et al.
704 1999; Erickson et al.1989) by dioxin (Fletcher et al., 2005; Moran et al., 2004) and estrogen
705 exposure (Ekman et al., 2008), as well as metabolic perturbation by exposure to pesticides
706 like endosulfan and chlorpyrifos (Demur et al., 2013; Wang et al., 2011).
707
708 The lipidomics data suggested that PAHs, similar to the pesticides and the contaminant
709 mixtures, perturbed steroid biosynthesis by elevating several cholesterol intermediates, and
710 thereby affecting steroid hormone biosynthesis. In benzo(a)pyrene and contaminant mixture
711 exposed cells, higher vitamin D3 levels (putatively identified) were detected when compared
712 to the other exposure groups. Given that fish can only acquire D3 vitamin via its feed, a time-
713 dependent reduction of vitamin D3 levels owing to cells metabolism of the vitamin, suggests
714 that vitamin D3 steroid biosynthesis has been inhibited by these contaminants (Lock et al.,
715 2010). Potent CYP1A inducers, like benzo(a)pyrene, have previously been reported to down-
716 regulate or inhibit estrogen receptor signalling (Kortenkamp, 2007; Yan et al., 2012).
717 However at the highest concentration of benzo(a)pyren (100 μM), VTG was significantly
718 induced, as shown for chlorpyrifos, which also appears to be a potent CYP1A inducer.
719
720 Despite phenanthrene's lack of lipidomic perturbation and effect on CYP3A expression
721 levels, the RT-qPCR analysis revealed that phenanthrene significantly elevated CYP1A at the
722 highest exposure concentration (100 μM), indicating that it is a weak CYP1A inducer.
723 Surprisingly, phenanthrene toxicity in fish therefore appears to be induced via the AhR as

724 compared to earlier findings in mammals where phenanthrene toxicity has been found to be
725 independent of the AhR induction (Pathiratne and Hemachandra, 2010; Johnson et al., 2008;
726 Wolinska et al., 2011). Weak CYP1A inducers have previously been found to act differently
727 in fish test systems possibly due to fish-specific CYP1A regulation (Søfteland et al., 2011)
728 with fish having more AhRs then mammals (Hahn and Hestermann, 2008), in addition to low
729 CYP2K/CYP2M and CYP3A induction abilities. In addition, VTG was highly elevated in
730 cells exposed to 100 μM of phenanthrene, with a FC of 10.9. A similar VTG response was not
731 detected in corresponding studies with zebrafish or medaka (Horng et al., 2009; Wolinska et
732 al., 2011). However, hydroxylated PAHs like 2-hydroxyphenanthrene, which have structural
733 similarities to E2, have been shown to possess estrogenic activity in estrogen-sensitive
734 reporter gene assays (ER-CALUX) (Wenger et al., 2009).
735
736 According to the lipidomics data, additivity appeared to be the dominant mixture effect
737 between the PAHs and the pesticides. The high level of overlap in lipidome perturbation
738 between the individual contaminants and contaminant mixtures, and the increased number of
739 perturbations induced by contaminant mixtures with high levels of pesticides, indicate that the
740 majority of changes in the lipidome induced by the contaminant mixtures represent the sum of
741 the individual contaminants. However, some synergistic activity between the compounds
742 cannot be ruled out. In line with earlier studies with potent CYP1A inducers (van den Berg et
743 al., 2006) and EDCs (Kortenkamp, 2007), the PLS interaction evaluation of the CYP1A and
744 FABP4 transcriptional data, confirmed that additivity was the dominant mixture effect caused
745 by the PAHs and pesticides. However, at high concentrations, synergistic interaction effects
746 were detected. In the contaminant mixture cell viability screening, at high concentrations
747 chlorpyrifos synergistically interacted with and potentiated endosulfan's cytotoxic response,
748 despite having no effect on cell viability alone. A similar synergistic effect on cell viability
749 reduction has previously been shown in Ehrlich ascites tumour cells from Swiss albino mice,
750 in which Thiram, at non-cytotoxic concentration, was found to potentiate the cell viability
751 reduction of endosulfan (Rana and Shivanandappa, 2010). In line with the cell viability
752 results, at high concentrations a synergistic effect between endosulfan and chlorpyrifos was
753 detected on the transcriptional down-regulation of CYP3A and FABP4. A similar additive (at
754 low concentrations) and synergistic response (at high exposure concentration) was reported in
755 an acetylcholinesterase activity inhibition study with juvenile coho salmon (*Oncorhynchus*
756 *kisutch*) exposed to a mixture composed of organophosphate and carbamate pesticides (Laetz

et al., 2009). A synergistic inhibition of cholinesterase has also been detected in great ramshorns *(Planorbarius corneus)* exposed to a binary mixture of chlorpyrifos and one organophosphate pesticide (Cacciatore et al., 2012). The mechanism behind the pesticides' synergistic effect on the down-regulation of CYP3A and FABP4 is, however, not known. CYP3A is an important contaminant biotransformation enzyme in addition to having a role in the metabolism of steroid hormones like testosterone (Kretschmer et al., 2005) and other lipids. The observed down-regulation of this transcript may therefore affect CYP3A-dependent biotransformation of contaminants and turnover of hormones and lipids in cells. This illustrates that risk assessment based on toxicological data from single-contaminant exposure studies can underestimate the impact of the mixture of new contaminants with different modes of action, like PAHs and pesticides, which may be introduced to farmed Atlantic salmon from feeds with high inclusion levels of vegetable oil.

5. Conclusions

Despite that the two PAHs benzo(a)pyrene and phenanthrene were associated with higher cell viability reduction potential the two pesticides endosulfan and chlorpyrifos caused the greatest lipidomics and transcriptomic perturbations. According to the lipidomics data, the two metabolic pathways most strongly affected by chlorpyrifos and endosulfan, contaminants that could be introduced in novel salmon feeds from plant-based ingredients, were fatty acid and steroid biosynthesis. These responses were to some extent confirmed by the transcriptomic data, which showed that biomarkers linked to endocrine disruption and lipid metabolism were affected. According to the current observations, the interaction effects between the contaminants could mostly be explained as an additive effect, however at high concentrations the contaminants acted in a synergistic manner.

Acknowledgments

The authors would like to thank Betty Irgens, Eva Mykkeltvedt and Synnøve Wintertun (NIFES) for their contribution with the experimental work. The LTQ FT Ultra used in this research was obtained, through the Birmingham Science City Translational Medicine: Experimental Medicine Network of Excellence project, with support from Advantage West Midlands (AWM). This work was funded by the Norwegian Research Council (NRC), Grant number 200506 and NIFES, Norway.

812

813

814

815

816

817

818 **References**

819 Abassi, Y.A., Xi, B., Zhang ,W., Ye, P., Kirstein, S.L., Gaylord, M.R., Feinstein, S.C., Wang,
820 X., Xu, X., 2009. Kinetic cell-based morphological screening: prediction of mechanism of
821 compound action and off-target effects. Chem Biol. 16(7), 712-23.
822
823 Atienzar, F.A, Tilmant, K., Gerets, H.H., Toussaint, G., Speeckaert, S., Hanon, E., Depelchin,
824 O., Dhalluin, S., 2011. The use of real-time cell analyzer technology in drug discovery:
825 defining optimal cell culture conditions and assay reproducibility with different adherent
826 cellular models. J Biomol Screen. 16(6), 575-87.
827
828 De Angelis, S., Tassinari, R., Maranghi, F., Eusepi, A., Di Virgilio, A., Chiarotti, F., Ricceri,
829 L., Venerosi Pesciolini, A., Gilardi, E., Moracci, G., Calamandrei, G., Olivieri, A.,
830 Mantovani, A., 2009. Developmental exposure to chlorpyrifos induces alterations in thyroid
831 and thyroid hormone levels without other toxicity signs in CD-1 mice. Toxicol Sci. 108(2),
832 311-9.
833
834 Ashad, N., Shabbir, G., Aleem, S., Arshad, M., 2007. Effects of α-tocopherol on liver
835 biochemistry of endosulfan intoxicated mice: A preliminary study. Asian J. Exp. Sci. 21(2),
836 239-46.
837
838 Babich, H., Borenfreund, E., 1987. Polycyclic aromatic hydrocarbon in vitro cytotoxicity to
839 bluegill BF-2 cells: mediation by S-9 microsomal fraction and temperature. Toxicol. Lett. 36,
840 107–16.
841
842 Babich, H., Sardana, M.K., Borenfreund, E., 1988. Acute cytotoxicities of polynuclear
843 aromatic hydrocarbons determined in vitro with the human liver tumor cell line, HepG2. Cell
844 Biol. Toxicol. 4, 295–309.
845
846 Babin, M.M., Tarazona, J.V., 2005. In vitro toxicity of selected pesticides on RTG-2 and
847 RTL-W1 fish cell lines. Environ Pollut. 135, 267–74.
848
849 Bandele, O.J., Santillo, M.F., Ferguson, M., Wiesenfeld, P.L., 2012. In vitro toxicity
850 screening of chemical mixtures using HepG2/C3A cells. Food Chem Toxicol. 50(5), 1653-9.
851
852 Benisek, M., Kubincova, P., Blaha, L., Hilscherova, K., 2011. The effects of PAHs and
853 N-PAHs on retinoid signaling and Oct-4 expression in vitro. Toxicol. Lett. 200(3), 169–75.

Berntssen, M.H., Giskegjerde, T.A., Rosenlund, G., Torstensen, B.E., Lundebye, A.K., 2007. Predicting World Health Organization toxic equivalency factor dioxin and dioxin-like polychlorinated biphenyl levels in farmed Atlantic salmon (Salmo salar) based on known levels in feed. Environ Toxicol Chem. 26(1), 13-23.

Berntssen, M.H.G., Julshamn, K., Lundebye, A.K., 2010. Chemical contaminants in aquafeeds and Atlantic salmon (Salmo salar) following the use of traditional- versus alternative feed ingredients. Chemosphere. 78, 637-46.

Black, J.A., Birge, W.J., Westerman, A.G., Francis, P.C., 1983. Comparative aquatic toxicology of aromatic hydrocarbons. Fund. Appl. Toxicol. 3, 353-8.

Bo, T.H., Dysvik, B., Jonassen, I., 2004. LSimpute: accurate estimation of missing values in microarray data with least squares methods. Nucleic Acids Res. 32(3), e34.

Bols, N.C., Dayeh, V.R., Lee, L.E.J., Schirmer, K., 2006. Use of fish cell lines in the toxicology and ecotoxicology of fish. Pescine cell line in environmental toxicology, in: Mommsen, T.P, Moon, T.W. (Eds.), Environmental toxicology: Biochemistry and molecular biology of fishes, vol.6. Elsevier, Amsterdam, pp. 43-84.

Booman, M., Borza, T., Feng, C.Y., Hori, T. S., Higgins, B., Culf, A., Léger, D., Chute, I.C., Belkaid, A., Rise, M., Gamperl, A.K., Hubert, S., Kimball, J., Ouellette, R.J., Johnson, S.C., Bowman, S., Rise, M.L., 2011. Development and experimental validation of a 20K Atlantic cod (Gadus morhua) oligonucleotide microarray based on a collection of over 150,000 ESTs. Mar Biotechnol. 13(4), 733-50.

Bouhifd, M., Bories, G., Casado, J., Coecke, S., Norlén, H., Parissis, N., Rodrigues, R.M., Whelan, M.P., 2012. Automation of an in vitro cytotoxicity assay used to estimate starting doses in acute oral systemic toxicity tests. Food Chem Toxicol. 50(6), 2084-96.

Braunbeck, T., Appelbaum, S., 1999. Ultrastructural alterations in the liver and intestine of carp Cyprinus carpio induced orally by ultra-low doses of endosulfan. Dis Aquat Organ. 36, 183-200.

Bravo, E., Cantafora, A., Cicchini, C., Avella, M., Botham, K. M., 1999. The influence of estrogen on hepatic cholesterol metabolism and biliary lipid secretion in rats fed fish oil. Biochim Biophys Acta. 1437, 367–77.

Breitling, R., Armrngaud, P., Amtmann, A., Herzyk, P., 2004. Rank products: a simple, yet powerful, new method to detect differently regulated genes in replicated microarray expoeriments. FEBS Lett. 573, 83-92.

Cabr´e, A., L´azaro,I., Girona,J., Manzanares,J.M., Marim´on, F., Plana,N., Heras, M., Masana, L., (2007). Fatty acid binding protein 4 is increased in metabolic syndrome and with thiazolidinedione treatment in diabetic patients. Atherosclerosis. 195, 150–8.

Cacciatore LC, Kristoff G, Verrengia Guerrero NR, Cochón AC., 2012. Binary mixtures of azinphos-methyl oxon and chlorpyrifos oxon produce in vitro synergistic cholinesterase inhibition in Planorbarius corneus. Chemosphere. 88(4), 450-8.

Celton, M., Malpertuy, A., Lelandais, G., de Brevern, A.G., 2010. Comparative analysis of missing value imputation methods to improve clustering and interpretation of microarray experiments. BMC Genomics. 11, 15.

Ceriotti, L., Ponti, J., Broggi, F., Kob., A., Drechsler, S., Thedinga, E., Colpo, P, Sabbioni, E., Ehret, R., Rossi, F., 2007. Real-time assessment of cytotoxicity by impedance measurement on a 96-well plate. Sensor Actuat B-Chem. 123(2), 769–78.

Deb, N., Das, S., 2012. Chlorpyrifos toxicity in fish: A review. Curr World Environ. 8(1), 1-7.
Demur, C., Métais, B., Canlet, C., Tremblay-Franco, M., Gautier, R., Blas-Y-Estrada. F, Sommer. C., Gamet-Payrastre, L., 2013. Dietary exposure to a low dose of pesticides alone of as a mixture: The biological metabolomic fingerprint and impact on hematopoiesis. Toxicology. 308, 74–87.

Gelboin, H.V., Huberman, E., Sachs, L., 1969. Enzymatic hydroxylation of benzopyrene and its relationship to cytotoxicity. Proc Natl Acad Sci. 64, 1188–94.

Dieterle, F., Ross, A., Schlotterbeck, G., Senn, H., 2006. Metabolite projection analysis for fast identification of metabolites in metabonomics. Application in an amiodarone study. Anal Chem. 78(11), 3551-61.

Donnelly, K.C., Naufal, Z.S., 2010. Toxic and Genotoxic Effects of Mixtures of Polycyclic Aromatic Hydrocarbon, in: Mumtaz, M. (Ed.), Principles and Practice of Mixtures Toxicology. DOI: 10.1002/9783527630196.ch20.

Ekman DR, Teng Q, Villeneuve DL, Kahl MD, Jensen KM, Durhan EJ, Ankley GT, Collette TW, (2008). Investigating compensation and recovery of fathead minnow (Pimephales promelas) exposed to 17alpha-ethynylestradiol with metabolite profiling. Environ Sci Technol. 42(11), 4188-94.

Erickson, S. K., Jaeckle, S., Lear, S. R., Brady, S. M., Havel, R. J., 1989. Regulation of hepatic cholesterol and lipoprotein metabolism in ethinylestradiol-treated rats. J Lipid Res. 30, 1763–71.

Fletcher, N., Wahlström, D., Lundberg, R., Nilsson, C.B., Nilsson, K.C., Stockling, K., Hellmold, H., Håkansson, H., 2005. 2,3,7,8-Tetrachlorodibenzo-p-dioxin (TCDD) alters the mRNA expression of critical genes associated with cholesterol metabolism, bile acid biosynthesis, and bile transport in rat liver: a microarray study. Toxicol Appl Pharmacol. 207(1), 1-24.

Fromberg, A., Hojgard, A., Duedahl-Olesen, L., 2007. Analysis of polycyclic aromatic hydrocarbons in vegetable oils combining gel permeation chromatography with solid-phase extraction clean-up. Food Addit. Contam., 24, 758-67.

Glover, C.N., Petri, D., Tollefsen, K.E., Jorum, N., Handy, R.D., Berntssen, M.H.G., 2007. Assessing the sensitivity of Atlantic salmon (Salmo salar) to dietary endosulfan exposure using tissue biochemistry and histology. Aquat Toxicol. 84, 346-55.

Grünfeld, H.T., Bonefeld-Jorgensen, E.C., 2004. Effect of in vitro estrogenic pesticides on human oestrogen receptor α and β mRNA levels. Toxicol Lett. 151, 467-80.

Hagve, T.A., Christpphersen, B.O. Böger, P., 1985. Norflurazon – an inhibitor of essential fatty acid desaturation in isolated liver cells. Lipids, 20(10), 719-22.

Hahn, M.E., Hestermann, E.V., 2008. Receptor-mediated mechanisms of toxicity, in: Di Giulio, D.E. Hinton (Eds.), The Toxicology of Fishes, Taylor and Francis Group, Boca Raton, FL, pp. 235–72.

Hawkins, S.A., Billiard, S.M., Tabash, S.P., Brown, R.S., Hodson, P.V., 2002. Altering cytochrome P4501A activity affects polycyclic aromatic hydrocarbon metabolism and toxicity in rainbow trout (Oncorhynchus mykiss). Environ Toxicol Chem. 21(9), 1845-53.

Hinton, D.E., Segner, H., Au, D.W.T., Kullman, S.W., Hardman, R.C., 2008. Liver toxicity, in: Di Giulio , Hinton, D.E. (Eds.), The toxicology of fishes, Taylor and Francis Group, Boca Raton, Florida, pp. 327-400.

Hong, F., Breitling, R., McEntee, C.W., Wittner, B.S., Nemhauser, J.L., Chory, J., 2006. RankProd: a bioconductor package for detecting differentially expressed genes in meta-analysis. Bioinformatics. 22(22), 2825-7.

Hori, T.S., Gamperl, A.K., Booman, M., Nash, G.W., Rise, M.L., 2012. A moderate increase in ambient temperature modulates the Atlantic cod (Gadus morhua) spleen transcriptome response to intraperitoneal viral mimic injection. BMC Genomics. 13, 431.

Horng, C.Y., Lin, H.C, Lee, W., 2009. A Reproductive Toxicology Study of Phenanthrene in Medaka (Oryzias latipes). Arch Environ Contam Toxicol. DOI 10.1007/s00244-009-9335-6

Hrydziuszko,O., Viant, M.R., 2012. Missing values in mass spectrometry based metabolomics: an undervalued step in the data processing pipeline. Metabolomics. DOI 10.1007/s11306-011-0366-4.

ISO, 2009. Biological evaluation of medical devices Part 5: Tests for in vitro cytotoxicity. International standard, ISO 10993-5:2009, 1-34.

Janesick, A., Blumberg,B., 2011. Minireview: PPARγ as the target of obesogens. J Steroid Biochem Mol Biol. 127, 4-8.

Jeffery, I.B., Higgins, D.G., Culhane, A.C., 2006. Comparison and evaluation of methods for generating differentially expressed gene lists from microarray data. BMC Bioinformatics. 26 (7), 359.

Jantzen, S.G., Sanderson, D.S., von Schalburg, K.R., Yasuike, M., Marass, F., Koop, B.F. (2011). A 44K microarray dataset of the changing transcriptome in developing Atlantic salmon (Salmo salar L.). BMC Res. Notes. 4, 88.

Jergentz, S., Mugni, H., Bonetto, C., Schulz, R., 2005. Assessment of insecticide contamination in runoff and stream water of small agricultural streams in the main soybean area of Argentina. Chemosphere. 61, 817-26.

Johnson, L.L, Arkoosh, M.R., Bravo, C.F., Collier, T.K., Krahn, M.M., Meador, J.P., Myers, M.S., Reichert, W.L., Stein J.E., 2008.The effects of polycyclic aromatic hydrocarbons in fish from Puget sound Washington, in: Di Giulio , Hinton, D.E. (Eds.), The toxicology of fishes, Taylor and Francis Group, Boca Raton, Florida, pp. 877-923.

Judson, R.S., Houck, K.A., Kavlock, R.J., Knudsen, T.B., Martin, M.T., Mortensen, H.M., Reif, D.M., Rotroff, D.M., Shah, I., Richard, A.M., Dix, D.J., 2010. In vitro screening of environmental chemicals for targeted testing prioritization: the ToxCast project. Environ Health Perspect. 118 (4), 485-92.

Kanehisa, M., Araki, M., Goto, S., Hattori, M., Hirakawa, M., Itoh, M., Katayama, T., Kawashima, S., Okuda, S., Tokimatsu, T., Yamanishi, Y., 2008. KEGG for linking genomes to life and the environment. Nucleic Acids Res., 36(Database issue), D480-4.

Kirwan, J.A., Broadhurst, D.I., Davidson, R.L., Viant, M.R., 2013. Characterising and correcting batch variation in an automated direct infusion mass spectrometry (DIMS) metabolomics workflow. Anal Bioanal Chem., 405(15), 5147-57.

Konkel, A., Schunck, W.H., 2011. Review: Role of cytochrome P450 enzymes in the bioactivation of polyunsaturated fatty acids. Biochim Biophys Acta. 1814, 210-22.

Kortenkamp, A., Altenburger,R., 2011. Toxicity from combined exposure to chemicals, in: van Gestel, C.A.M., Jonker M.J., Kammenga, J.E., Laskowski, R., Svendsen, C. (Eds.), Mixture Toxicity: Linking Approaches from ecological and human toxicology. Taylor and Francis Group, New York, USA, pp. 95-119.

Kortenkamp, A., 2007. Ten years of mixing cocktails: A review of combination effects of endocrine-disrupting chemicals. Environ Health Perspect. 115(1), 98-105.

Krøvel, A.V., Søfteland, L., Torstensen, B.E., Olsvik, P.A., 2010. Endosulfan in vitro toxicity in Atlantic salmon hepatocytes obtained from fish fed either fish oil or vegetable oil. Comp Biochem Physiol C Toxicol Pharmacol. 151(2), 175-86.

Laetz, C. A., Baldwin, D.H., Collier, T.K., Hebert, V., Stark, J.D., Scholz, *N.L.*, 2009. The Synergistic Toxicity of Pesticide Mixtures: Implications for Risk Assessment and the Conservation of Endangered Pacific Salmon. Environ Health Perspect. 117(3), 348-53.

LeBlanc G.A., Norria, D.O., Kloas W., Kullman, S.W., Baldwin, W.S., Greally, J.M., 2012. Draft detailed review paper state of the science on novel in vitro and in vivo screening and testing methods and endpoints for evaluating endocrine disruptors. OECD Environment, Health and Safety Publications, Series on Testing and Assessment, 178, 1-213.

Li, T., Chiang, J.Y.L., 2009. Regulation of Bile Acid and Cholesterol Metabolism by PPARs. PPAR Research, 501739. 10.1155/2009/501739.

Lin, C.Y., Anderson, B.S, Phillips, B.M., Peng, A.C., Clark, S., Voorhees, J., Wu, H.D. I., Martin, M.J., McCall, J., Todd, C.R., Hsieh, F., Crane, D:, Viant, M.R., Sowby, M.L., Tjeerdema, R.S., 2009. Characterization of the metabolic actions of crude versus dispersed oil in salmon smolts via NMR-based metabolomics. Aquat Toxicol. 95, 230–8.

Lock, E.-J., Waagbø, R., Wendelaar Bonga, S., Flik, G., 2010. The significance of vitamin D for fish: a review. Aquacult Nutrit. 16(1), 100–16.

Marchis, D., Ferro, G.L., Brizio, P., Squadrone, S., Abete, M.C., 2012. Detection of pesticides in crops: A modified QuEChERS approach. Food Cont. 25, 270-3.

Merchant, M., Morrison,V., Santostefano, M., Safe, S., 1992. Mechanism of action of aryl hydrocarbon receptor antagonists: inhibition of 2,3,7,8-tetrachlorodibenzo-p-dioxin-induced CYP1A1 gene expression. Arch Biochem Biophys, 298(2), 389-94.

Michalik, L., Wahli, W., 2008. PPARs mediated lipid signaling in inflammation and cancer. PPAR Research, 134059. doi: 10.1155/2008/134059.

Moghaddam, M., Motoba, K., Borhan, B., Pinot, F., Hammock, B.D., 1996. Novel metabolic pathways for linoleic and arachidonic acid metabolism. Biochim Biophys Acta. 1290(3), 327-39.

Monteiro, J., Askarian, F., Nakamura, M.T., Moghadasian, M.H., Ma, D.W., 2013. Oils rich in α-linolenic acid independently protect against characteristics of fatty liver disease in the Δ6-desaturase null mouse. Can J Physiol Pharmacol. 91(6), 469-79.

Moran, F.M., Hendrickx, A.G., Shideler, S., Overstreet, J.W., Watkins, S.M., Lasley, B.L., 2004. Effects of 2,3,7,8-tetrachlorodibenzo-p-dioxin (TCDD) on fatty acid availability and neural tube formation in cynomolgus macaque, Macaca fascicularis. Birth Defects Res B Dev Reprod Toxicol. 71(1), 37-46.

Nácher-Mestre, J., Serrano, R., Portolés, T., Berntssen, M.H., Pérez-Sánchez, J., Hernández, F., 2014. Screening of pesticides and polycyclic aromatic hydrocarbons in feeds and fish tissues by gas chromatography coupled to high-resolution mass spectrometry using atmospheric pressure chemical ionization. J Agric Food Chem. 62(10):2165-74.

NIFES, 2014. Seafood data, Undesirables. http://www2.nifes.no/index.php?page_id=137&lang_id=2.

Ortiz-Zarragoitia, M., Cajaraville, M.P., 2005. Effects of selected xenoestrogens on liver peroxisomes, vitellogenin levels and spermatogenic cell proliferation in male zebrafish. Comp Biochem Physiol C Toxicol Pharmacol.141(2), 133-44.

Parkinson, A., Ogilvie, B.W., 2008. Biotransformation of Xenobiotics, in: Klaassen, C.D. (ed), Casarett and Doull's Toxicology: The basic science of poisons, McGraw-Hill, Inc., New York, USA, pp.161-304.

Pathiratne, A., Hemachandra, C.K., 2010. Modulation of ethoxyresorufin O-deethylase and glutathione S-transferase activities in Nile tilapia (Oreochromis niloticus) by polycyclic aromatic hydrocarbons containing two to four rings: implications in biomonitoring aquatic pollution. Ecotoxicology. 19(6), 1012-8.

Payne, T.G., Southam, A.D., Arvanitis, T.N., Viant, M.R., 2009. A signal filtering method for improved quantification and noise discrimination in fourier transform ion cyclotron resonance mass spectrometry-based metabolomics data. J Am Soc Mass Spectrom. 20(6), 1087-95.

Panigrahy, D., Kaipainen, A., Greene, E.R., Huang, S., 2010. Cytochrome P450-derived eicosanoids: the neglected pathway in cancer. Cancer Metastasis Rev., 29(4), 723-35.

Peraza, M.A., Burdick, A.D., Marin, H.E., Gonzalez, F.J., Peters, J.M., 2006. The toxicology of ligands for peroxisome proliferator-activated receptors (PPAR). Toxicol Sci. 90(2), 269-95.
Rana, I., Shivanandappa, T., 2010. Mechanism of potentiation of endosulfan cytotoxicity by thiram in Ehrlich ascites tumor cells. Toxicol in Vitro. 24, 40-4.

SCF, 2002. Opinion of the Scientific Committee on Food on the risks to human health of Polycyclic Aromatic Hydrocarbons in food. SCF/CS/CNTM/PAH/29 http://europa.eu.int/comm/food/fs/sc/scf/index_en.html.

Schroeder, A., Mueller, O., Stocker, S., Salowsky, R., Leiber, M., Gassmann, M., Lightfoot, S., Menzel, W., Granzow, M., Ragg, T., 2006. The RIN: an RNA integrity number for assigning integrity values to RNA measurements. BMC Mol Biol. 7, 3.

Segner, H., Braunbeck, T., 2003. End points for in vitro toxicity testing with fish cells, in: Mothersill, C., Austin, B. (eds.), In vitro methods in aquatic toxicology. Springer, Berlin, Heidelberg, pp. 77-142.

Seruto, C., Sapozhnikova, Y., Schlenk, D., 2005. Evaluation of the relationships between biochemical endpoints of PAH exposure and physiological endpoints of reproduction in male California Halibut (Paralichthys californicus) exposed to sediments from a natural oil seep. Mar Environ Res., 60(4), 454-65.

Schirmer, K., Dixon, D.G., Greenberg, B.M., Bols, N.C., 1998. Ability of 16 priority PAHs to be directly cytotoxic to a cell line from the rainbow trout gill. Toxicology. 1998 127(1-3), 129-41.

Southam, A.D., Payne, T.G., Cooper, H.J., Arvanitis, T.N., Viant, M.R., 2007. Dynamic range and mass accuracy of wide-scan direct infusion nanoelectrospray fourier transform ion cyclotron resonance mass spectrometry-based metabolomics increased by the spectral stitching method. Anal Chem. 79(12), 4595-602.

Søfteland, L., Petersen, K., Stavrum, A.K., Wu, T., Olsvik, P.A., 2011. Hepatic in vitro toxicity assessment of PBDE congeners BDE47, BDE153 and BDE154 in Atlantic salmon (Salmo salar L.). Aquat Toxicol. 105(3-4), 246-63.

Teixeira, V.H., Casal, S., Oliveira, M., 2007. PAHs content in sunflower, soybean and virgin olive oils: Evaluation in commercial samples and during refining process. Food Chem., 104, 106-12.

Tellmann, G., 2006. The E-Method: a highly accurate technique for gene-expression analysis. Nature Meth. 3, doi:10.1038/nmeth894.

Terra, X., Quintero,Y., Auguet T., Porras, J.A., Herna´ndez, M., Sabench, F., Aguilar, C., Luna1, A.M., del Castillo, D., Richart,C., 2011. FABP 4 is associated with inflammatory markers and metabolic syndrome in morbidly obese women. Eur J Endocrinol. 164, 539-54.

Torstensen, B.E., Frøyland, L., Lie, Ø., 2001. Lipider, in: Waagbø. R., Espe., M., Hamre, K., Lie. Ø., (Eds), Fiskeernæring. Kystnæringen forlag og bokklubb AS, Dreggen, Bergen, Norway. pp.57-76.

Torstensen, B.E., Nanton, D.A., Olsvik, P.A., Sundvold, H. and Stubhaug, I., 2009. Gene expression of fatty acid binding proteins (FABPs), fatty acid transport proteins (cd36 and FATP) and β-oxidation related genes in Atlantic salmon (Salmo salar L.) fed fish oil or vegetable oil. Aquacult Nutrit. 15(4), 440-51.

Van Den Berg, M., Birnbaum, L.S., Denison, M., De Vito, M. Farland, W., Feeley, M., Fiedler, H., Hakansson, H., Hanberg, A., Haws, L., Rose, M., Safe, S., Schrenk, D., Tohyama, C., Tritscher, A. Tuomisto, J., Tysklind, M., Walker, N., Peterson, R. E., 2006. The 2005 world health organization reevaluation of human and mammalian toxic equivalency factors for dioxins and dioxin-like compounds. Toxicol Sci. 93(2), 223-41.

van der Oost, R., Beyer, J., Vermeulen, N.P,E., 2003. Fish bioaccumulation and biomarkers in environmental risk assessment: a review. Environ Toxicol Pharmacol. 13, 57-149.

VanScoy, A.R., Lin, C.Y., Anderson, B.S., Philips, B.M., Martin, M.J., McCall, J., Todd, C.R., Crane, D., Sowby, M.L., Viant, M.R., Tjeerdema, R.S., 2010. Metabolic responses produced by crude versus dispersed oil in Chinook salmon pre-smolts via NMR-based metabolomics. Ecotoxicol Environ Saf. 73, 710–17.

Vandesompele, J., Preter, K.D., Pattyn, F., Poppe, B., Roy, N.V., Paepe, A.D., Speleman, F., 2002. Accurate normalization of real-time quantiative RT-PCR data by geometric averaging of multiple internal control genes. Genome Biol. 3 (7), Research0034.1-0034.11.

Viant, M.R., Rosenblum, E.S., Tieerdema, R.S., 2003. NMR-based metabolomics: a powerful approach for characterizing the effects of environmental stressors on organism health. Environ Sci Technol. 37(21), 4982-9.

Viswanath, G., Chatterjee, S., Dabral, S., Nanguneri, S.R., Divya, G., Roy, P., 2010. Anti-androgenic endocrine disrupting activities of chlorpyrifos and piperophos. J Steroid Biochem Mol Biol. 120(1), 22-9.

Walum, E., Hedander, J., Garberg, P., 2005. Research perspectives for pre-screening alternatives to animal experimentation: on the relevance of cytotoxicity measurements, barrier passage determinations and high throughput screening in vitro to select potentially hazardous compounds in large sets of chemicals. Toxicol Appl Pharmacol. 207 (2 Suppl), 393-7.

Wang, H.P., Liang, Y.J., Zhang, Q., Long, D.X., Li, W., Li, L., Yang, L., Yan, X.Z., Wu, Y.J., 2011. Changes in metabolic profiles of urine from rats following chronic exposure to anticholinesterase pesticides. Pestic Biochem Physiol. 101, 232-39.

Weber, J., Halsall, C.J., Muir, D., Teixeira, C., Small, J., Solomon, K., Hermanson, M., Hung, H., Bidleman, T., 2010. Endosulfan, a global pesticide: a review of its fate in the environment and occurrence in the Arctic. Sci Total Environ. 408(15), 2966-84.

Wenger D, Gerecke AC, Heeb NV, Schmid P, Hueglin C, Naegeli H, Zenobi R. 2009. In vitro estrogenicity of ambient particulate matter: contribution of hydroxylated polycyclic aromatic hydrocarbons. J Appl Toxicol. 29(3), 223-32.

Wold, S., 1978. Cross-validatory estimation of the number of components in factor and principal components models. Technometrics. 20 (4), 397-405.

Wold, S., Ruhe, A., Wold, H., Dunn III, W.J., 1984. The collinearity problem in linear regression. The partial least squares (PLS) approach to generalized inverses. SIAM J. Sci. and Stat. Comput. 5, 735-743.

Wolinska, L. Brzuzan,P., Woêny, M., Góra2, M.Łuczynski, M.K., Podlasz,P., Kolwicz,S., Piasecka, A., 2011. Preliminary study on adverse effects of phenanthrene and its methyl and phenyl derivatives in larval zebrafish, Danio rerio. Environ biotechnol. 7 (1), 26-33.

Wood, A.W., Janz, D.M., Van Der Kraak, G.J., 2006. Cell death: Investigation and application in fish toxicology, in: Mommsen, T.P, Moon, T.W. (Eds.), Environmental toxicology Biochemistry and molecular biology of fishes vol. 6, pp.303-28.

Xia, M., Huang, R., Witt, K.L., Southall, N., Fostel, J., Cho, M.H., Jadhav, A., Smith, C.S., Inglese, J., Portier, C.J., Tice, R.R., Austin, C.P., 2008. Compound cytotoxicity profiling using quantitative high-throughput screening. Environ Health Perspect. 116(3), 284-91. doi: 10.1289/ehp.10727.

Yan, Z., Lu, G., He, J., 2012. Reciprocal inhibiting interactive mechanism between the estrogen receptor and aryl hydrocarbon receptor signaling pathways in goldfish (Carassius auratus) exposed to 17β-estradiol and benzo[a]pyrene. Comp Biochem Physiol C Toxicol Pharmacol., 156(1), 17-23.

Yokoyama, Y., Nimura, Y., Nagino, M., Bland, K.I., Chaudry, I.H., 2005. Role of thromboxane in producing hepatic injury during hepatic stress. Arch Surg. 140(8), 801-7.

Abbreviations

Acidic ribosomal protein (ARP)

Analysis of variance (ANOVA)

Aryl hydrocarbon receptor (AhR)

Cell index (CI)

Crossing point (CT)

Cytochrome P450 1A (CYP1A)

Dimethyl sulfoxide (DMSO)

Elongation factor 1 AB (EF1AB)

Epoxide hydrolase (sEH)

Estrogen receptor (ER)

Ethoxyresorufin O-deethylase activity (EROD)

Fatty acid binding protein 4 (FABP4)

Fish serum (FS)

Fold change (FC)

Games-Howell (GH)

Genomic Research in All Salmonids Project (cGRASP)

Goodness of fit (R^2).

Goodness of prediction (Q^2),

Kyoto Encyclopedia of Genes and Genomes (KEGG)

Mean normalized expression (MNE)

Microtubule-associated proteins 1A/1B light chain 3B precursor (MAP1LC3B)

No-amplification control (nac)

Normalized cell index (NCI)

No-template control (ntc)

Nuclear magnetic resonance spectroscopy (NMR)

Partial Least Squares Discriminant Analysis (PLS-DA)

Percentage of false positives (PFP)

Peroxisome proliferator activated receptor γ (PPARγ)

Peroxisome proliferator-activated receptor α (PPARα)

Persistent organic environmental pollutants (POPs)

Photomultiplier tube settings (PMTs)

Polycyclic aromatic hydrocarbons (PAHs)

Principal Component Analysis (PCA)

Quality control (QC)

Quantitative real-time RT-PCR (real-time qPCR)

Rainbow trout gill cells (RTgill-W1)

Rainbow trout gonadal (RTG-2)

Rainbow trout liver (RTL-W1)

Reverse transcription (RT)

Reverse transcription (RT)

Reverse transcription polymerase chain reaction (RT-PCR)

Selected ion monitoring (SIM)

Tetrahydrofurandiols (THF-diols)

Transcription factor SOX-4 (SOX4)

Triacylglycerols (TAG)

Vitellogenin (VTG)

Highlights

Atlantic salmon primary hepatocytes were used to screen for interaction effects caused by PAHs and pesticides.

Lipidomic and transcriptomic profiling suggested perturbation of lipid metabolism and endocrine disruption.

The pesticides gave the strongest responses, despite having less effect on cell viability than the PAHs.

The primary mixture effect was additive.

At high concentrations, the pesticides acted synergistic by decreasing cell viability and down-regulating CYP3A and FABP4.

Tables

Table 1: Overview over the different concentration (µM) combinations used for the various pesticides and PAHs used in the factorial design for microarray and RT-qPCR evaluation.

Exposure no.	Benzo(a)pyrene	Phenanthrene	Chlorpyrifos	Endosulfan
1	1	1	1	1
2	100	1	1	1
3	1	100	1	1
4	100	100	1	1
5	1	1	100	1
6	100	1	100	1
7	1	100	100	1
8	100	100	100	1
9	1	1	1	100
10	100	1	1	100
11	1	100	1	100
12	100	100	1	100
13	1	1	100	100
14	100	1	100	100
15	1	100	100	100
16	100	100	100	100
17	50.5	50.5	50.5	50.5
18	DMSO	DMSO	DMSO	DMSO

Table 2: PCR primers, GenBank accession numbers, amplicon sizes and efficiency.

Gene	Accession no.	Forward primer (5' - 3')	Reverse primer (5' - 3')	Product size (bp)	Efficiency
CYP1A	AF364076	TGGAGATCTTCCGGCACTCT	CAGGTGTCCTTGGGAATGGA	101	2.06
PPARA	DQ294237	TCTCCAGCCTGGACCTGAAC	GCCTCGTAGACGCCGTACTT	58	2.05
CYP3A	DQ361036	ACTAGAGAGGGTCGCCAAGA	TACTGAACCGCTCTGGTTTG	146	2.1
SOX4	NP_001167115	GAGGCCGATGAACGCTTTC	AGCGCTTGCCCAGTCTCTT	110	2.1
FABP4	BT125322	CCGCCGACGACAGAAAAA	TTTTGCACAAGGTTGCCATTT	61	2.03
MAP1LC3B	NP_001239285	TGCCCATCCTGGATAAAACC	GCCATTCACCAGCAGGAAGA	125	1.93
VTG	C065R146	GACTTCGCCATCAGCCTTTC	GCCACGGTCTCCAAGAAGTCT	110	2.14
EF1AB	AF321836	TGCCCCTCCAGGATGTCTAC	CACGGCCCACAGGTACT	59	2.13
UBA52	GO050814	TCAAGGCCAAGATCCAGGAT	CGCAGCACAAGATGCAGAGT	139	1.9
B-ACTIN	BG933897	CCAAAGCCAACAGGGAGAA	AGGGACAACACTGCCTGGAT	92	2.04

Table 3: Table of metabolic pathways perturbed by exposing salmon hepatocyte cells to contaminants. The extent of perturbation was measured by collating the mass features for each contaminant that had changed significantly compared to the control and mapping these as putatively annotated empirical formulae onto metabolic pathways as listed by KEGG (http://www.genome.jp/kegg/). The percentage perturbation of the pathway can then be estimated based on the percentage of the original pathway detected that was significantly different. Figures in red denote the greatest perturbation seen in that pathway for the individual contaminants.

KEGG Pathway*	Theoretical pathway information		Percentage of the putatively annotated empirical formula that are perturbed by the contaminant				
	Number of empirical formulae listed in KEGG pathway	Number of putatively annotated empirical formulae detected by DIMS lipidomics	Endosulfan	Chlorpyrifos	Benzo(a)pyrene	Phenanthrene	Mixture
Primary bile acid biosynthesis	29	7	86	71	57	14	86
Biosynthesis of unsaturated fatty acids	42	12	0	83	0	0	83
Steroid biosynthesis	19	5	80	40	60	20	80
Retinol metabolism	9	5	0	60	20	0	80
Linoleic acid metabolism	9	6	0	83	0	0	67
Vitamin digestion and absorption	29	6	33	50	17	0	67
Steroid hormone biosynthesis	45	9	56	33	22	0	44
alpha-Linolenic acid metabolism	25	6	17	50	0	0	33
Phenylalanine metabolism	47	9	0	22	0	0	33
Arachidonic acid metabolism	19	5	0	40	40	20	20

*Only pathways with 5 or more unique empirical formulae detected and 2 or more empirical formulae significantly perturbed have been included. Pathways unique to plant or microbial metabolism have been excluded.

Table 4: Top rank product list of differently expressed features with PFP below 10% in Atlantic salmon hepatocytes exposed to contaminant mixture 4[a] (N=5).

Exposure	Gene	ID	Microarray	
			Fold change	PFP[A]
Mixture 4	Vitellogenin precursor	C065R146	13.19	0.000
Mixture 4	Vitellogenin precursor	C207R010	7.72	0.005
Mixture 4	UNKNOWN	C175R143	5.59	0.013
Mixture 4	Microtubule-associated proteins 1A/1B light chain 3B precursor	C099R165	9.54	0.017
Mixture 4	Endonuclease domain-containing 1 protein precursor	C001R110	4.66	0.027
Mixture 4	Pleiotropic regulator 1	C126R053	6.88	0.028
Mixture 4	Retinoic acid receptor RXR-gamma-B	C159R064	7.71	0.028
Mixture 4	Transcription factor SOX-4	C084R080	4.05	0.029
Mixture 4	Actin-related protein 2/3 complex subunit 1A	C080R051	4.59	0.033
Mixture 4	Vitellogenin precursor	C088R103	2.87	0.045
Mixture 4	UNKNOWN	C033R065	1.16	0.047
Mixture 4	Ferritin, middle subunit	C023R056	3.97	0.048
Mixture 4	Zinc finger FYVE domain-containing protein 1	C131R039	4.41	0.051
Mixture 4	Pre-mRNA cleavage complex II protein Clp1	C124R050	5.46	0.064
Mixture 4	UNKNOWN	C072R085	3.05	0.081
Mixture 4	Neuropeptide B precursor	C080R062	3.05	0.081
Mixture 4	UNKNOWN	C105R067	2.85	0.095

[a]Contaminant mixture 4 is composed of benzo(a)pyrene and phenanthrene (100 µM), endosulfan and chlorpyrifos (1 µM).

Table 5: Scaled and centered PLS regression coefficient models for different genes measured in primary Atlantic salmon hepatocytes exposed to chlorpyrifos (Chl), endosulfan (End), benzo(a)pyrene (Ben) and phenanthrene (Phe) using mean normalized expression (MNE) and factorial design. The combined effects identified with contour plot analysis for the different models are presented in the response column. The specific contaminants that contributed to a particular combined effect like additivity, synergism or antagonism are specified in parentheses behind the identified combined response in the response column. PLS plots of genes where only one contaminant was responsible for the observed response is indicated in the response column by naming the contaminant responsible for the effect.

Gen	PLS scaled and centered coefficients	Response
CYP1A	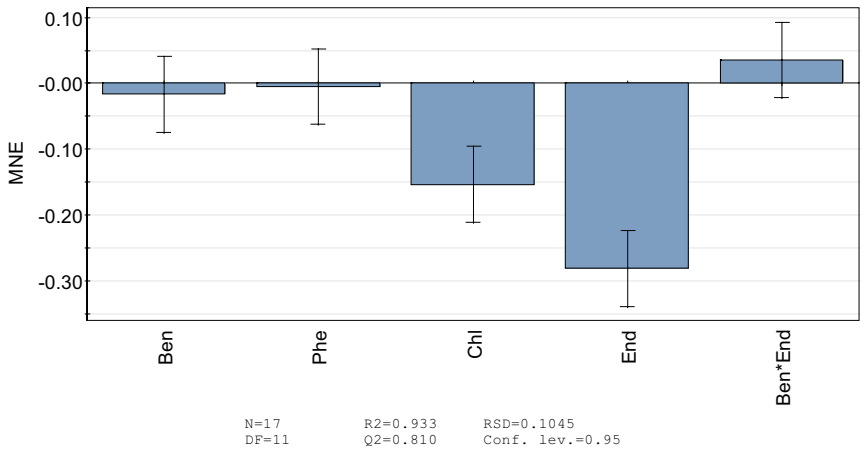	Additivity (Chl+End)
CYP3A	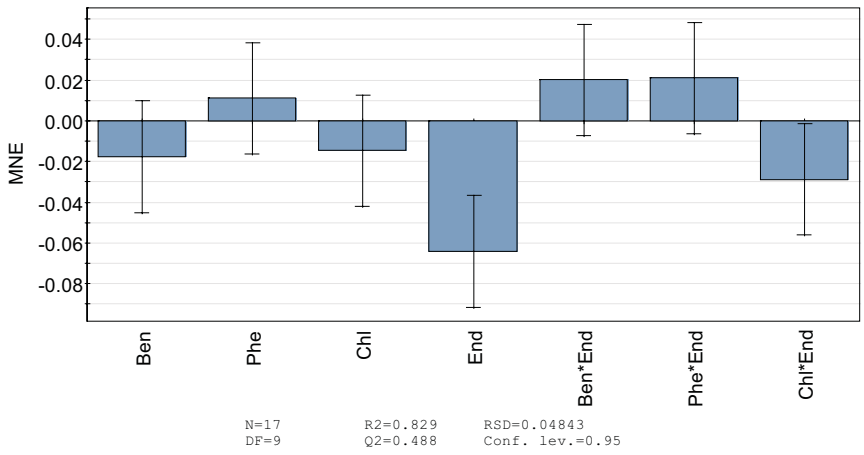	Synergism (Chl+ End)

VTG

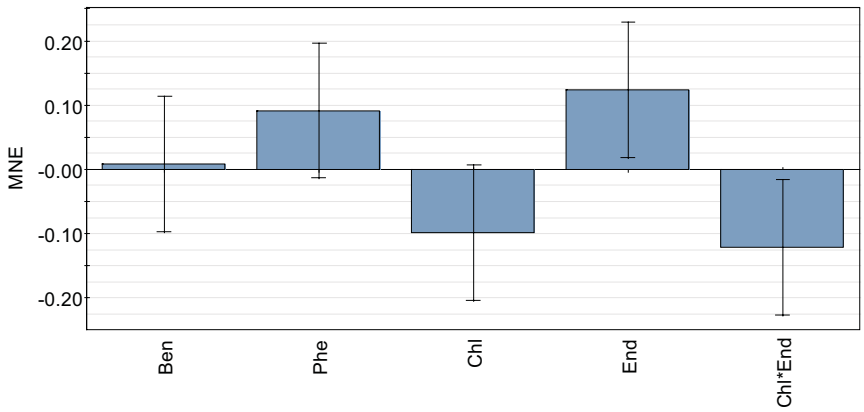

N=17 R2=0.658 RSD=0.1911
DF=11 Q2=0.470 Conf. lev.=0.95

End

FBP4

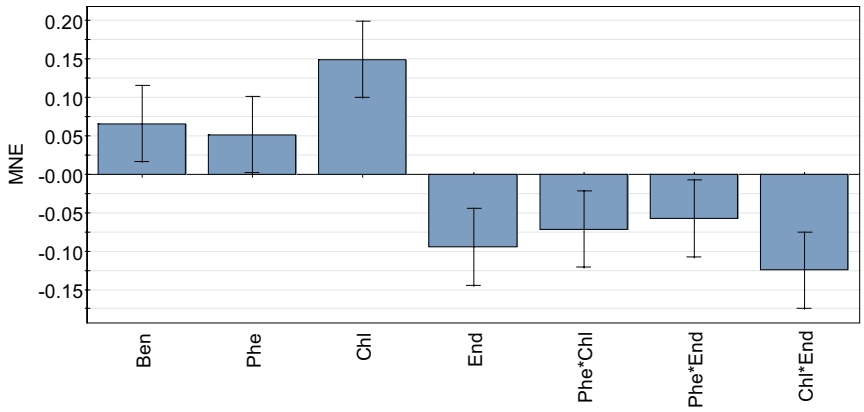

N=17 R2=0.934 RSD=0.08822
DF=9 Q2=0.694 Conf. lev.=0.95

Additivity (Ben, Phe and Chl)

Synergism (Chl+ End)

Antagonism (Phe+ End)

PPARα

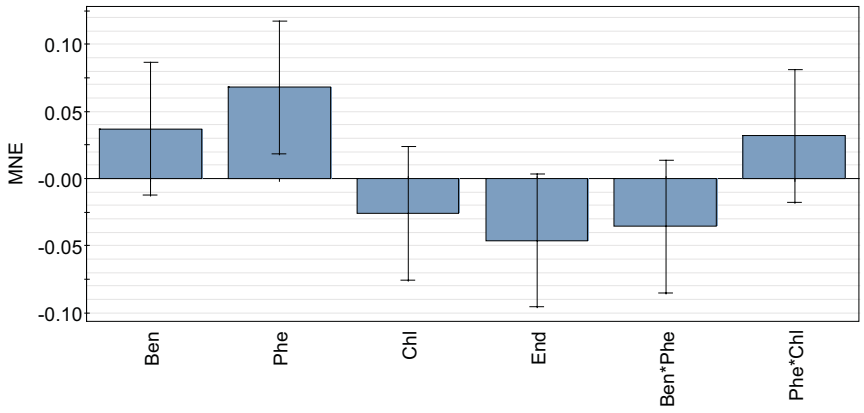

N=17 R2=0.692 RSD=0.08893
DF=10 Q2=0.436 Conf. lev.=0.95

Phe

MAP1L C3B

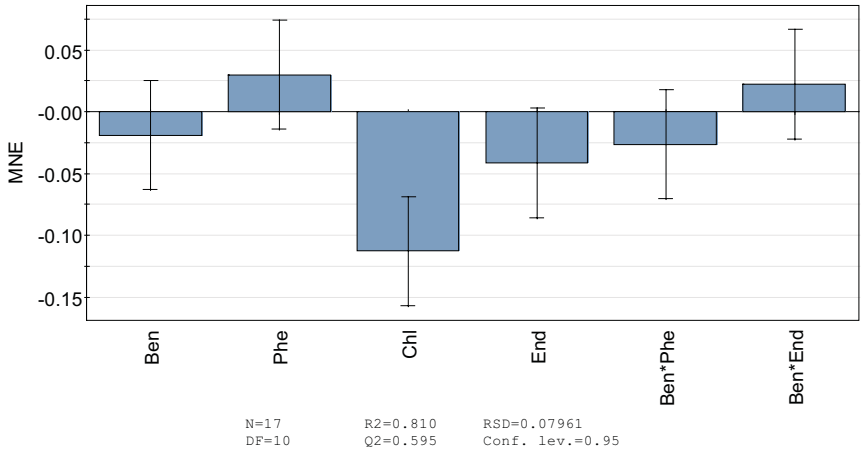

Chl

SOX4

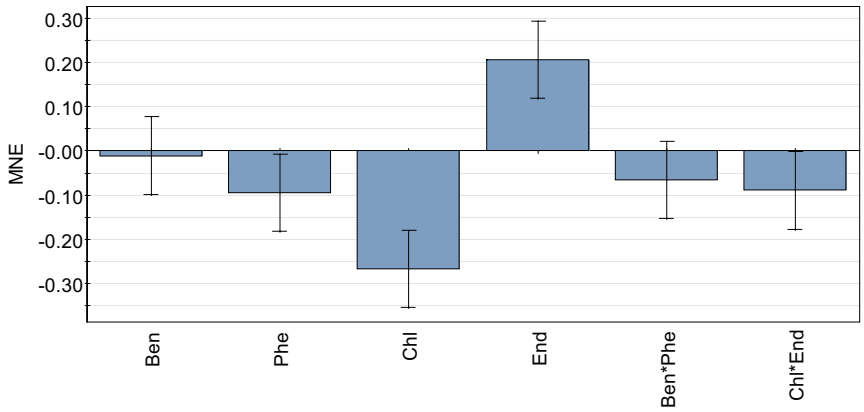

Additivity (Chl+Phe)

Figures

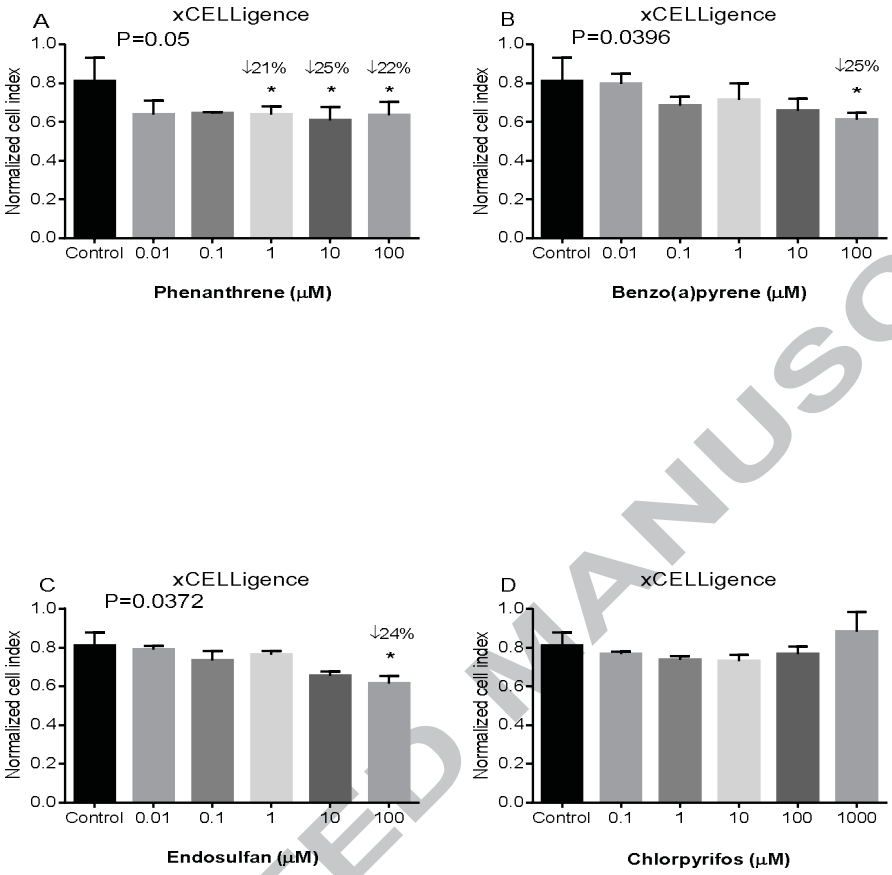

Fig. 1: Dose-response curves for Normalized cell index (NCI) values obtained for primary Atlantic salmon hepatocytes (N=3) exposed to (A) phenanthrene (B) benzo(a)pyrene, (C) endosulfan, (D) and chlorpyrifos. The values represent the mean±SE of three replicates (N=3). The analyses showed significant difference between the control (DMSO 0.4%) and the exposed group indicated by * (p=0.05).

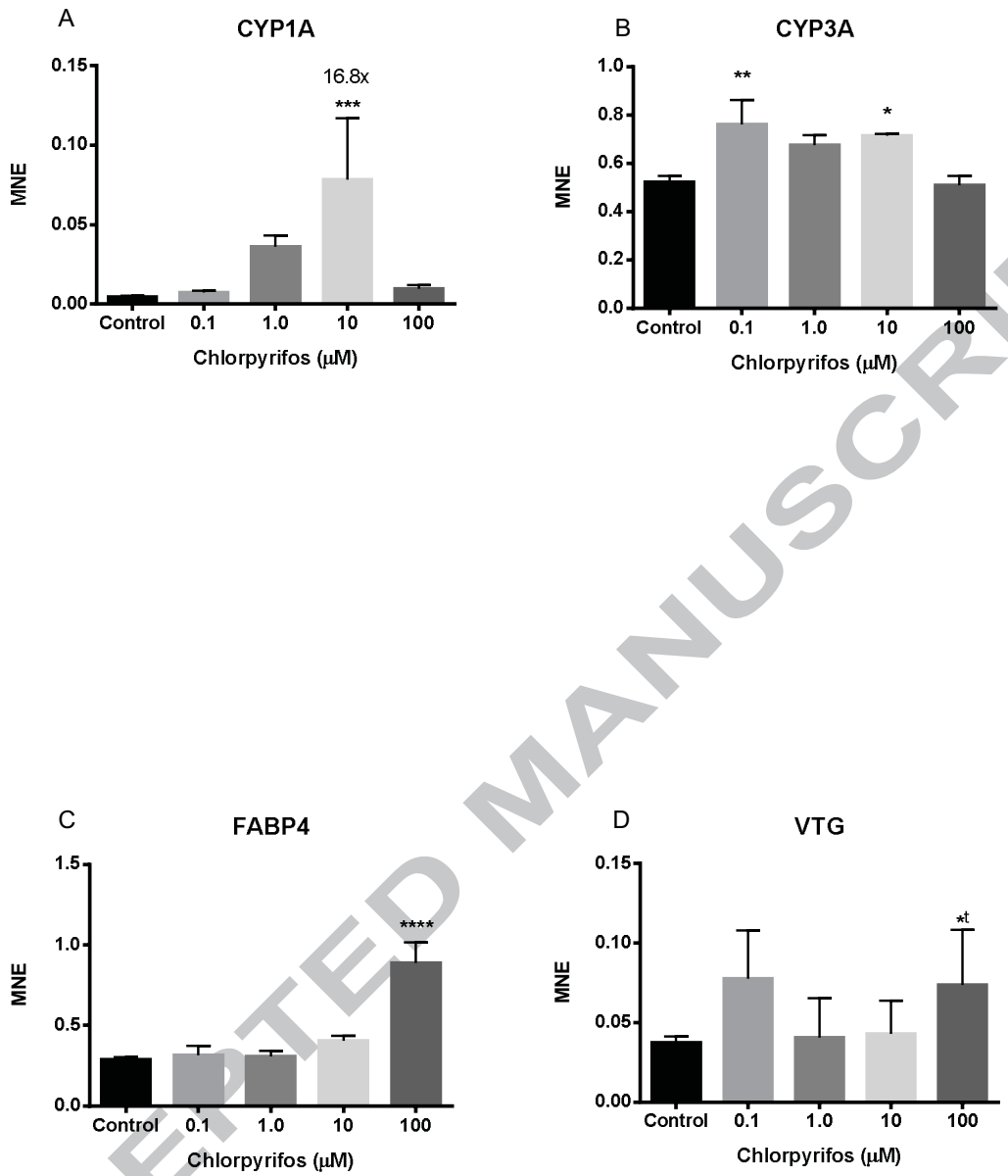

Fig. 2: Dose-response curves for A) CYP1A, B) CYP3A, C) FABP4, D) VTG, using normalized expression (MNE) values, obtained for primary Atlantic salmon hepatocytes exposed to chlorpyrifos and the DMSO control (0.4%). The values represent the mean±SE of three replicates (N=3). The ANOVA analyses showed significant difference between the control and the exposed group indicated by **** (P=0.0001), *** (p=0.001), ** (p=0.01) and * (p=0.05). The Students't-test analyses showed significant difference between the control (DMSO 0.4%) and the exposed group indicated by $*^{t}$ (p=0.05).

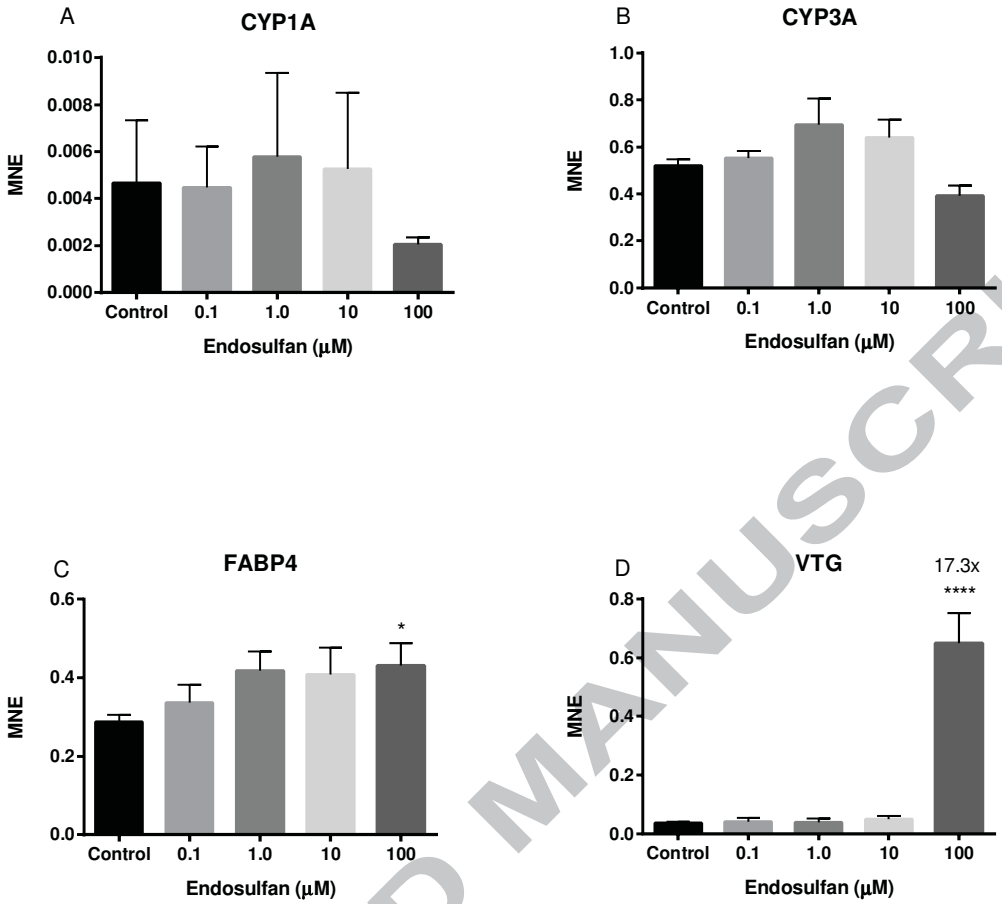

Fig. 3: Dose-response curves for A) CYP1A, B) CYP3A, C) FABP4, D) VTG, using normalized expression (MNE) values, obtained for primary Atlantic salmon hepatocytes exposed to endosulfan and the DMSO control (0.4%). The values represent the mean±SE of three replicates (N=3). The ANOVA analyses showed significant difference between the control and the exposed group indicated by **** (P=0.0001) and * (p=0.05).

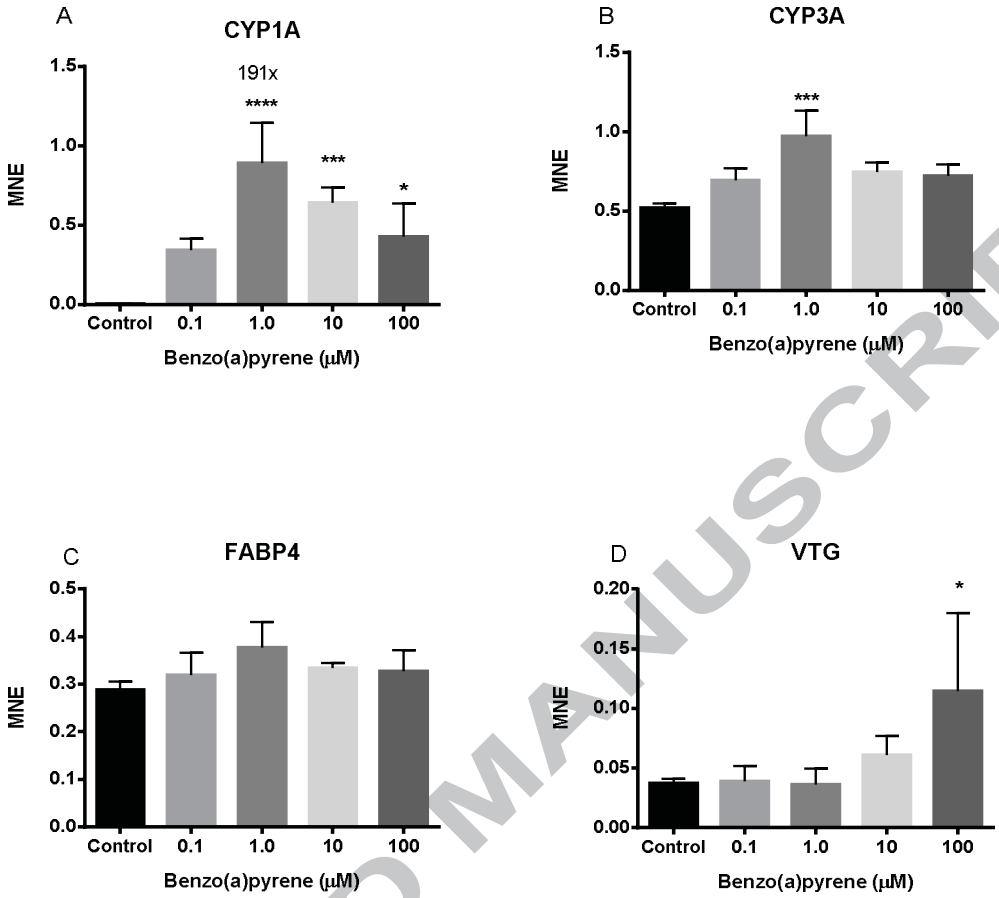

Fig. 4: Dose-response curves for A)CYP1A, B)CYP3A, C)FABP4, D) VTG, using normalized expression (MNE) values, obtained for primary Atlantic salmon hepatocytes exposed to benzo(a)pyrene and the DMSO control (0.4%). The values represent the mean±SE of three replicates (N=3). The ANOVA analyses showed significant difference between the control and the exposed group indicated by **** (P=0.0001), *** (p=0.001) and * (p=0.05).

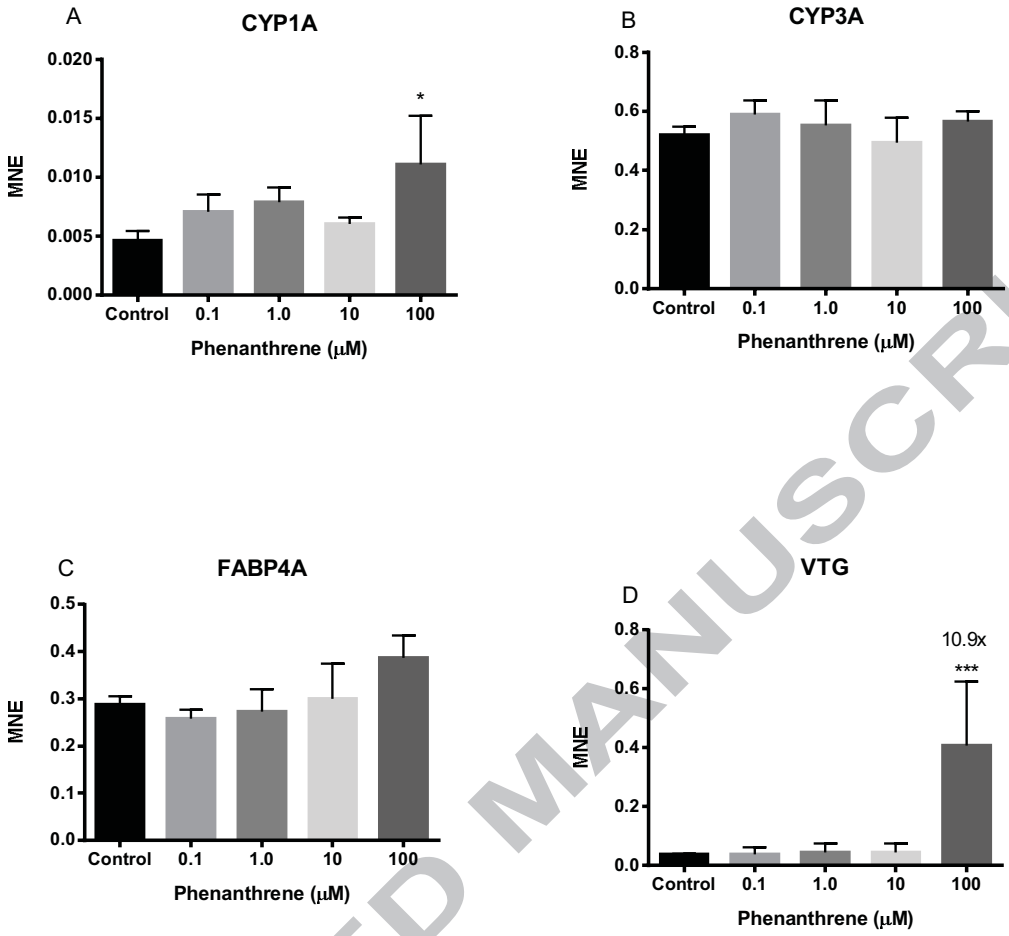

Fig. 5: Dose-response curves for A) CYP1A, B) CYP3A, C) FABP4 D) VTG, using normalized expression (MNE) values, obtained for primary Atlantic salmon hepatocytes exposed to phenanthrene and the DMSO control (0.4%). The values represent the mean±SE of three replicates (N=3). The ANOVA analyses showed significant difference between the control and the exposed group indicated by *** (p=0.001) and * (p=0.05).

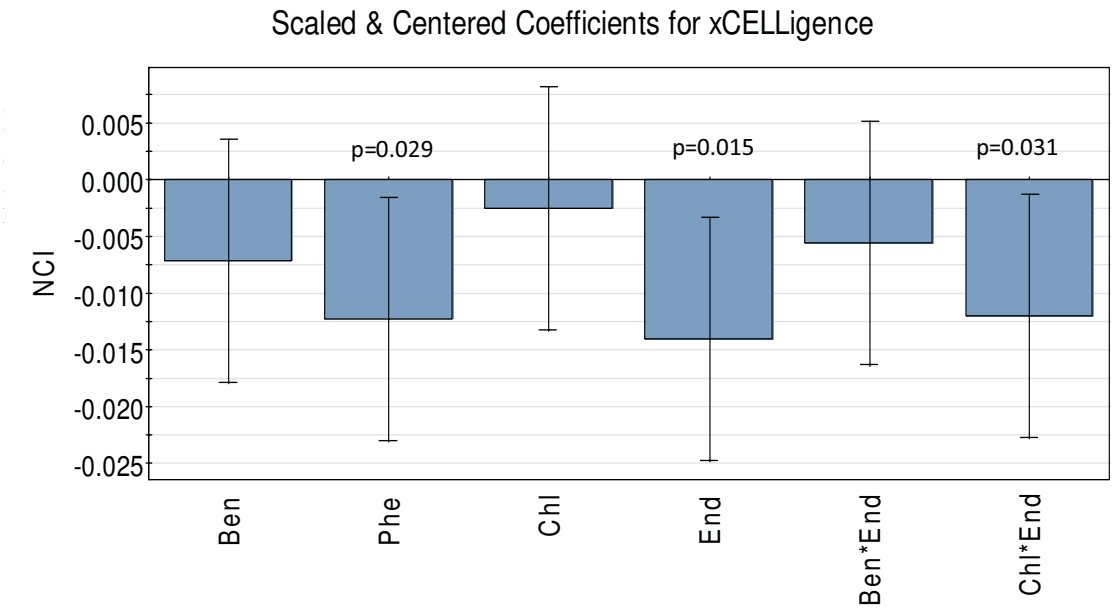

Fig. 6: Scaled and centered PLS regression coefficients with 95% confidence intervals for Normalized cell index (NCI) levels measured in primary Atlantic salmon hepatocytes exposed to benzo(a)pyrene, phenanthrene, chlorpyrifos and endosulfan accordingly to the factorial design (N=5). The model is based on 17 experimental objects, and had one PLS component. The model was good (R^2=0.7 and Q^2=0.4), containing four linear terms and two interaction terms.

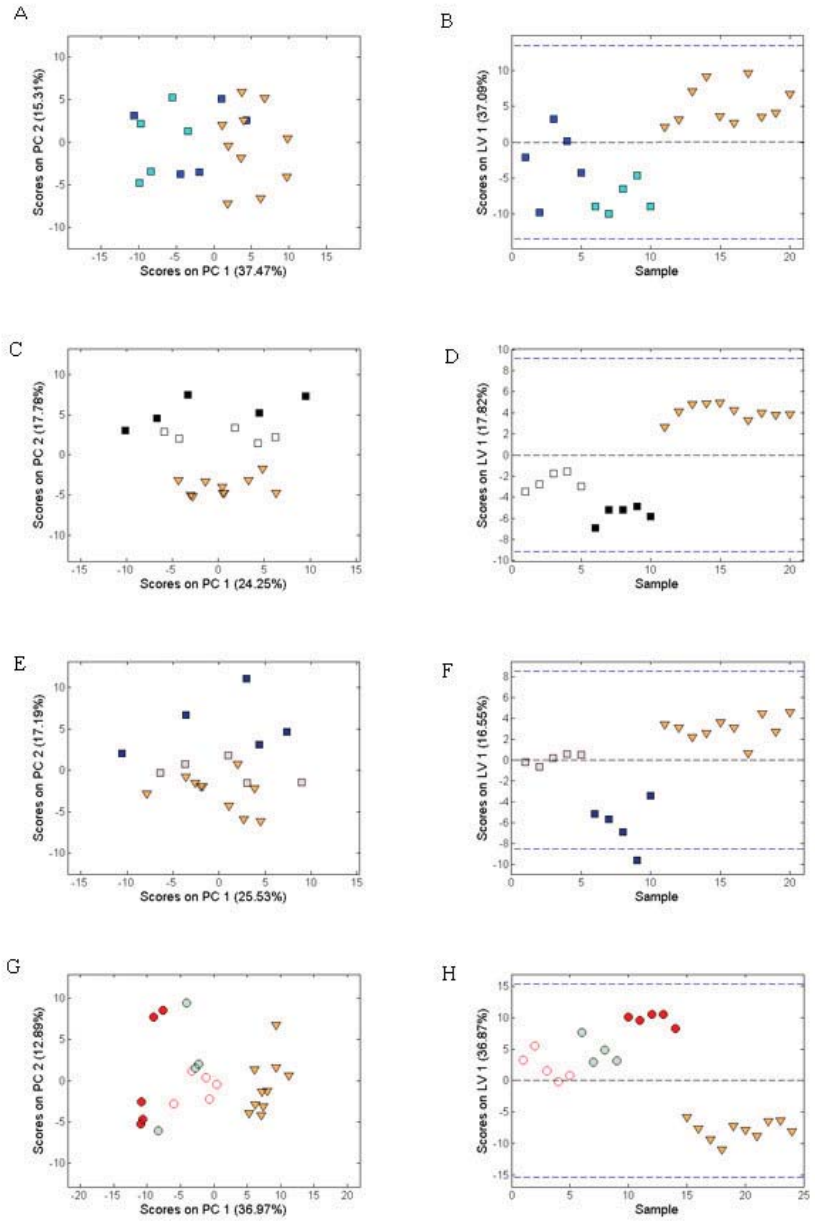

Fig. 7: PCA and PLSDA scores plots for lipidomics. PCA (left hand column) and PLSDA (right hand column) scores plots data from salmon hepatocyte cell cultures treated with chlorpyrifos (A and B), endosulfan (C and D), benzo(a)pyrene (E and F), or a mixture (I and J) of four contaminants (benzo(a)pyrene, chlorpyrifos, endosulfan and phenanthrene) at one of three different doses or DMSO control. One sample from the contaminant mixture 4 class has been removed as an outlier in the DIMS lipidomics data. Key to treatments: control(▽) low dose (1 µM) chlorpyrifos, (■) high dose (100 µM) chlorpyrifos (□), low dose endosulfan (□), high dose endosulfan (■), low dose benzo(a)pyrene

(□), high dose bezo(a)pyrene (■) or mixtures 1 (○), 4 (◍) and 16 (●) of the four contaminants.

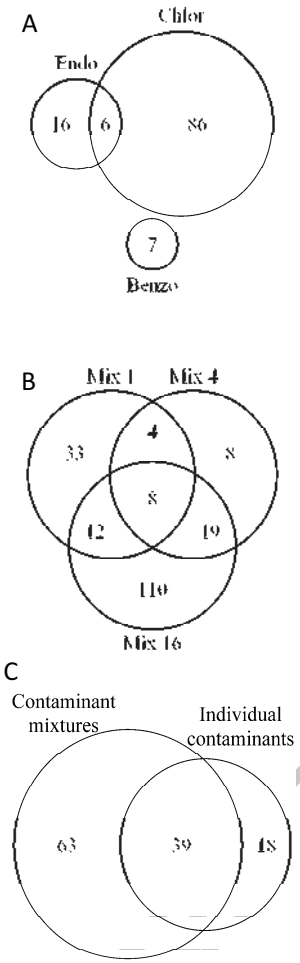

Fig. 8: Venn diagrams to summarise the significant mass features by ANOVA with Games-Howell post-hoc testing. The significant mass features between high dose individual contaminants versus control do not show much overlap (A). Phenanthrene was excluded from this analysis since statistical tests revealed there was only one mass feature significantly different from the control after FDR correction. This mass feature was also significantly different in endosulfan compared to the control. (B) The Venn diagram displays the difference in significant mass features between different contaminant mixes and the control, and (C) displays the overlapping mass features that were significant in any individual contaminant and the contaminant mixes.

A

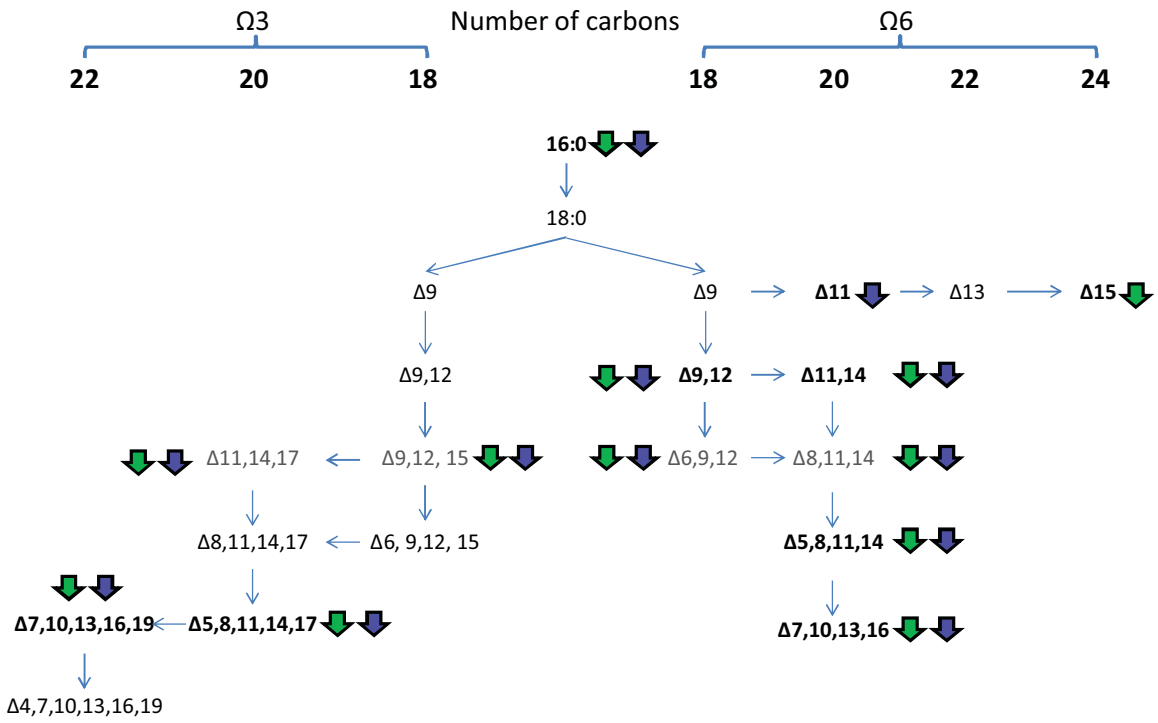

B

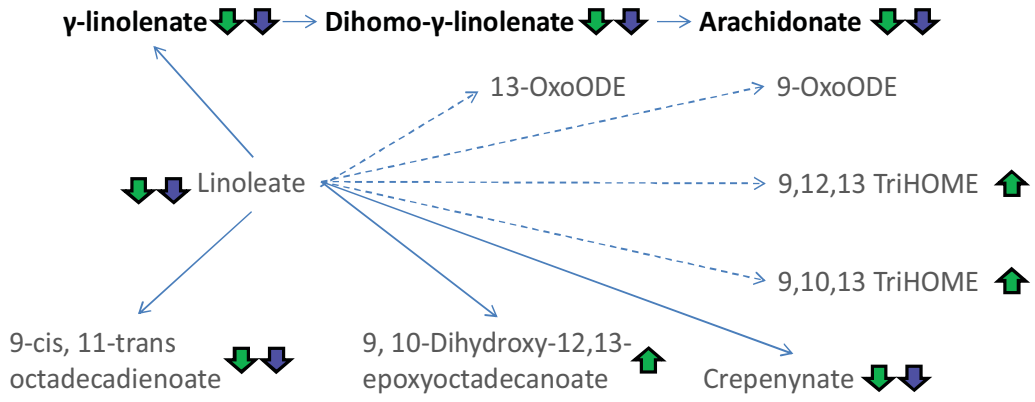

C

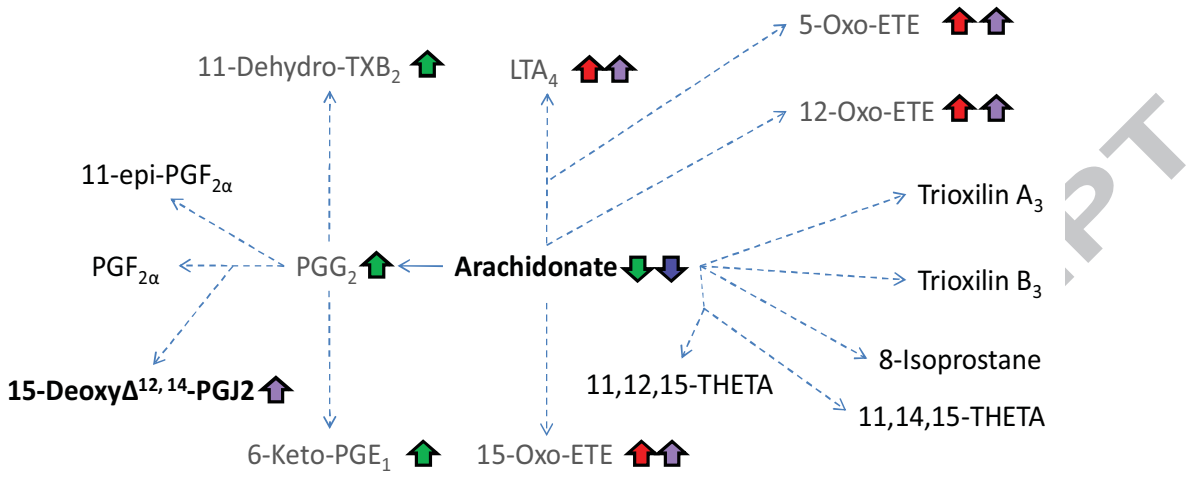

D

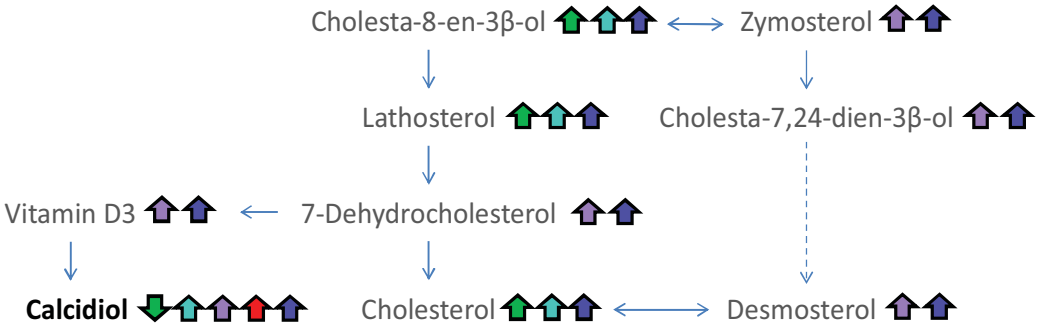

Fig. 9: Examples of metabolic pathways with significantly changing putatively annotated empirical formulae mapped onto them for each contaminant. All pathways have been reduced to show only the metabolites detected by direct infusion lipidomics. Block arrows demonstrate a significant fold increase or decrease following exposure to the contaminants in relation to the control group Key ( ) chlorpyrifos ( ) endosulfan ( ) phenanthrene ( ) benzo(a)pyrene ( ) contaminant mixture. Dotted arrows represent two or more reactions between the metabolites of interest and metabolites in grey font indicate that potentially multiple metabolites of the same *m/z* exist in this pathway. Biosynthesis of unsaturated fatty acids pathway (A) and the linoleic pathway (B) shows perturbations only when chlorpyrifos or a contaminant mixture is used. By contrast, the arachidonic acid metabolism pathway (C) and the steroid pathway (D) (reduced to show only the section of interest) appear disrupted by a much greater range of contaminants.